An-Najah National University

Faculty of Graduate Studies

Synthesis and Characterization of a Polymeric Nanoparticles of a Potent Anticancer Agent (Combretastatin)

By

Muna Hassan

Supervisors

Prof. Abdel Naser Zaid

Co-supervisor

Dr. Alaaldin Alkilany

This Thesis is Submitted in Partial Fulfillment of the Requirements for the Degree of Master in Pharmaceutical sciences, Faculty of Graduate Studies, An- Najah National University, Nablus, Palestine.

2018

Synthesis and Characterization of a Polymeric Nanoparticles of a Potent Anticancer Agent (Combretastatin)

By

Muna Hassan

This Thesis was defended successfully on / /2018 and approved by:

Defense Committee Members	**Signature**
– **Prof. Abdel Naser Zaid/ Supervisor**	**…….**
– **Dr. Numan Malkieh / External Examiner**	**……....**
– **Dr. Asma Ridwan/ Internal Examiner**	**……..…….**

Dedication

All praise to Allah the Almighty.

This study is dedicated with gratitude

To

My beloved Mother who always left me up and encouraged me.

To

My lovely family and Friends.

To

Anyone who reads and appreciates this study.

Thank you from all my heart

Acknowledgment

All praise to Allah the Almighty, for giving me the blessing, the strength, the chance, and endurance to complete this study and complete my master's degree.

I dedicate this achievement to my mother, thank you for always being there to lift me up and encourage me. You are my strength through all the tribulations, always been and always will be.

I would like to express my sincere gratitude to my amazing supervisors Professor Abdel Naser Zaid for his time, generous guidance, patient, and encouragement through the whole study.

Especial and cordially thanks to Dr. Samer Abu Lateefeh for his scientific support and precious continuous help. I believe that his contribution was essential to complete this scientific effort.

Also, I could not finish this study without the help and support of Dr. Alaa Aldin Alkilany and Reem Alabbassi, for that I thank you all.

I wish to express my deep gratitude tow hom are behind the scenes, my lovely supporting family, and my great friends for that they have encouraged me all through the way. Without your support, my master's degree achievement may not have been done.

Thank you from all my heart.

Muna Hassan

الإقرار

أنا الموقع أدناه مقدم الرسالة التي تحمل العنوان:

تركيب و توصيف الجسيمات البولمريه بحجم النانو لمركب فعال ضد السرطان (كومبريتاستاتين)

أقر بأن ما اشتملت عليه هذه الرسالة إنما في نتاج جهدي الخاص, باستثناء ما تمت الإشارة إليه حيثما ورد, وأن هذه الرسالة ككل, أو أي جزء منها لم يقدم من قبل لنيل أية درجة علمية أو بحث علمي أو بحثي لدى أي مؤسسة تعليمية أو بحثية أخرى.

Declaration

The work provided in this thesis, unless otherwise referenced, is the researcher's own work, and has not been submitted elsewhere for any other degree or qualification.

Student's name: **اسم الطالب:**

Signature: **التوقيع:**

Date: **التاريخ:**

Table of contents

List of Tables

List of Figures

List of abbreviations

Symbol	Abbreviation
ACN	Acetonitrile
AIC	Akaike Information Criterion
AIF	Apoptosis inducing factor
API	Active pharmaceutical ingredient
ATP	Adenosine 5′-triphosphate
β	Beta
°C	Celsius
CA4	Combretastatin
CA4P	CA4 triphosphate
CGM	Culture growth medium
CNTs	Carbone nanotubes
CO_2	Carbone dioxide
CR	Controlled released
DCM	Dichloromethane
DMEM	Dulbecco's Modified Eagle Medium
DMSO	Dimethyl sulfoxide
DDIW	Double de-ionized water
DDS	Drug delivery system
DL	Dug loading
DLS	Dynamic light scattering
DNA	Deoxyribonucleic acid
DOX	Doxorubicin
Drug loading	Drug loading
EE	Encapsulation efficiency
EEM	Emulsion evaporation method
EPR	Enhanced permeability retention
ERDFs	Extended-release dosage forms
EtOAc	Ethylacetate
FBS	Fetal bovine serum
H	Hour
HCl	Hydrogen chloride
H_2O	Water
HPLC	High performance liquid chromatography
HUVEC	Human umbilical vein endothelial cells
IUPAC	International Union of Pure and Applied Chemistry
IVR	*In vitro* release study
M	Molar
µg	Microgram

µl	Microliter
Ml	Milliliter
MDA	microtubules distrusting agents
Mg	Milligram
MNP	Mononuclear phagocyte
MRDFs	Modified release dosage forms
MTA	Microtubules targeting agents
MTX	Methotrexate
mV	Mili Volte
MW-CNTs	Multi walled-Carbonenanotubes
MWCO	Molecular weight cut off
NaCl	Sodium chloride
NaOH	Sodium hydroxide
NC	Nanocapsule
Ng	Nanogram
Nm	Nanometer
NMR	Nuclear magnetic resonance
NP	Nanoparticle
NPM	Nanoprecipitation method
NS	Nanospheres
O/W	Oil in water
PBS	Phosphate buffer saline
PDI	Poly-dispersity index
PEG	Poly-ethylene glycol
PLGA	Poly(lactic acid-co-glycolic acid)
PLG-g-PEG	pegylated poly (glutamic acid)
PNP	Polymeric nanoparticles
PVA	Poly vinyl alchohol
R^2	Linear regression
RGD	Arginine-glycin-aspartic acid
RPM	Round per minute
Kda	Kilo Dalton
SAR	Structural activity relationship
SD	Standard deviation
SLS	Sodium lauryl sulfate
SR	Sustained release
SW-CNTs	Single walled-Carbone nanotubes
TEM	Transmission electron microscope
UK	United kingdom
URPA	Urocanylpullulan
USA	United States of America

VDA	vascular disrupting agents
VIGF	vascular endothelial growth factor
UV	Ultra violet
Vis	Visible
WHO	World Health Organization
W/O	Water in oil
(W/O/W)	Water in oil in water

Synthesis and Characterization of a Polymeric Nanoparticles of a Potent Anticancer Agent (Combretastatin)

By
Muna Hassan
Supervisor
Prof. Abdel Naser Zaid
Co-Supervisor
Dr. Alaaldin Alkilany

Abstract

Background: Pharmaceutical nanotechnology is an emerging technology that proved its effectiveness in decreasing the side effects and improving the therapeutic outcomes of chemotherapeutic drugs. Combretastatin (CA4) is natural and potent antitubuline chemotherapeutic agent but it showed cardiotoxicity. **Purpose:** The aim of this research was to formulate and characterizeCA4 polymeric nanoparticles (NPs), to assess its release kinetic, and to evaluate the *in vitro* cytotoxic activity of the obtained NPs.

Method: CA4 was synthesized using Perkin reaction. Nano-precipitation and emulsion evaporation methods were used to produce the desired NPs. The obtained NPs were characterized for shape, particle size, zeta-potential, encapsulation efficiency% (EE%), drug loading% (DL%), and drug release. Cytotoxicity and IC_{50} of the free CA4and the loaded NPs were determined using two cancer cell lines Caco-2 and HeLa. **Results**: Emulsion evaporation method was capable to produce spherical shaped CA4 loaded NPs with EE% 50.84%, DL% 1.13%, mean average particle size 203.25 nm, and zeta-potential -38.50mV.The NPs showed sustained release pattern. Korsmeyer-Peppas was adopted to describe the release

mechanism of CA4 from our NPs, with n value higher than 1, which indicates a Super case II transport. *In vitro* cytotoxicity on Caco-2 and HeLa cells demonstrated better cytotoxic and IC_{50} of CA4 loaded NPs than the free CA4.

Conclusion:CA4 loaded polymeric NPs were successfully produced and showed satisfactory characteristics such as EE%, particle size and shape, zeta potential, and sustained release pattern. In addition, an improvement in the cytotoxic and IC_{50} of CA4 loaded NPs was demonstrated. This suggests that these NPs could be used to improve the safety, effectiveness, and patient compliance. However, *in vivo* studies should be conducted to prove these interesting findings.

Chapter One
Introduction

1.1 Cancer

Cancer is becoming one of the scariest diseases for human being. It is considered as the second cause of death worldwide, after cardiovascular diseases [1]. According to the cancer report, about 14.1 million people were expected to develop cancer annually [2], while WHO states that 8.2 million deaths were related to cancer in 2012 and increased to 8.8 million in 2015 [3]. Cancer disease or neoplasm is characterized by uncontrolled growth of abnormal cells that may invade and spread to surrounding tissues and organs [3]. There are more than 100 types of cancer. Treatment depends on the type and stage of malignancy which includes surgery, chemotherapy, and radiotherapy. Early detection and treatment would improve the outcome of the therapy and reduce patient suffering [4, 5]. Problems in the selectivity of the traditional chemotherapeutic agents (cytotoxic drugs) cause several unwanted side effects. Accordingly, drug selectivity is the main factor in the selection of chemotherapeutic agents [4, 6]. Chemotherapeutic or cytotoxic agents refer to any agent that kills or stop cancer cell division, generally through inhibition of microtubules, DNA and protein synthesis, and other mechanisms.

1.2 Nanopharmaceuticals

Nanotechnology is the science of managing and manufacturing material substance at the colloidal state in order to produce new products, devices, and systems. Nanopharmaceuticals are the pharmaceutical products that

have been designed by applying various principles of nanotechnology. Drug particles or drug products at the colloidal size range (1 to 1000 nm) demonstrated very interesting and novel properties that yield improved drug or product performances such as increasing the efficacy and safety of the drug, improving the medical imaging and medical devices, and other applications [7]. Several nanopharmaceutical products are now available in the pharmaceutical and medical market such as doxorubicin liposome injection, amphotericin B liposome injection [7]. In addition, nanotechnology has emerged in the last years as a noninvasive technique in the treatment and diagnosis of cancer [8, 9]. In fact, several scientific efforts are oriented toward the increase of selectivity and efficacy of drugs especially in the treatment of cancer. In this contest, selective targeting of the anticancer drugs toward tumor cells would increase the therapeutic index of the drugs. This can be done by using suitable drug carries or vehicles that deliver the drug specifically to the target organ or tissue and saving the normal cells from unwanted targeting [9]. The nature of the cancer tissue is different from healthy tissues. In fact, this tissue is leaky, immature, rapidly growing. In addition, the vascularity of the endothelial cells, with impaired lymphatic drainage and defect on the basement membrane compared to the normal blood vessel that contain complete endothelial cells with the tight junction, therefore, this results in accumulation of polymeric nanoparticles (PNPs) loaded with an anticancer drug in tumor cells [10, 11]. Moreover, the active targeting shifts the PNPs toward cancer cells which in turn called enhanced permeability retention (EPR) [10, 12]. Accordingly, nanoparticles (NPs) are considered drug carriers that carry anticancer drug specifically toward tumor cells with

numerous features as their size range in the nano-scale. Moreover, an increase in water solubility of poorly water-soluble drugs may result in improvement in their pharmacokinetic profile and bioavailability, protecting the drug from degradation, so improving the stability of the drug and shelf life, and increasing the biological permeability of the drugs improving the targeting and bioavailability of the bioactive molecules [7, 8, 13, 14].

1.3 Types of Pharmaceutical NPs

1.3.1 Liposomes

These products are small sized spherical shape of mono or multi layers of phospholipids. They are considered promising drug delivery systems (DDS) for a wide range of drugs due to their low toxicity, biocompatibility, site-specific targeting, hydrophobic and hydrophilic nature. They are composed of phospholipid layers that enclosed an aqueous media inside; as a result, water-soluble molecules can be trapped in this area while hydrophobic drugs are immersed in the lipophilic area of the phospholipid layer while amphipathic drug partition between two layers [7, 9].

1.3.2 Carbon nanotubes (CNTs)

CNTs are hollow cylindrical tubes made of carbon atoms. Depending on the number of the hollow tubes two types of CNTs were found, single-walled- CNTs (SW-CNTs) which are composed of a rape of one layer of graphene sheet while multi-walled- CNTs (MW-CNTs) which are made of

many layers of graphene sheets to produce a concentric cylindrical shape [15, 16]. Pristine CNTs are practically insoluble in any solvent. However, an increase in their solubility can be achieved when they functionalized. In addition, they become able to carry or conjugate with a wide range of molecules such as peptides, nucleic acids, and therapeutic drugs to deliver them inside the cells [16]. This can suggest the use of CNTs in the medical field in treating cancer, gene therapy, vaccination, and other medical purposes [16, 17].

1.3.3 Nanomicelles

These are defined as nanoscopic structure molecules composed of amphiphilic co-polymer with a hydrophobic core and hydrophilic shell. In this nano-structure, the water-insoluble drug is placed in the hydrophobic core, while the water-soluble one is located on the outer hydrophilic area. Usually, a process of micellization of the amphiphilic-polymers is used to produce these nanomicelles. They usually have a spherical shape with particle size range between 10-100nm depending on the polymer used. Poorly water-soluble drugs can be encapsulated into the micelles by physical or chemical methods. In the chemical methods, the drug is subjected to chemical binding with the polymer, while in the physical method the drugs are uploaded into the micelles by selective partitioning between the core and the shell during the process of micellization. Several advantages can be obtained using micelles as a DDS. These include an increase in the drug solubility of poorly water-soluble drugs, increase in

the drug stability, achieving controlled and extended release of the drug, and selective targeting to a specific organ [18].

1.3.4 Polymeric nanoparticles (PNPs)

PNPs are spherical colloidal dispersion with a size range from 10 to1000nm composed of large biocompatible and biodegradable polymers. The drug is usually loaded by adsorption, conjugation, or encapsulated within or onto the polymeric matrix. The PNPs can be obtained using amphiphilic polymers that contain hydrophobic and hydrophilic portions, which in aqueous solution spontaneously form a spherical shape giving an excellent and stable structure with minimized interfacial energy [19].

1.3.4.1. Types of PNPs

According to the used preparation method, two types of PNPs could be obtained, nanocapsules (NC) or nanospheres (NS). In the case of NC, the encapsulated compound is surrounded by a polymer and encapsulated in the hydrophobic core, while in the nanospheres structure, the drug is dispersed homogeneously in the polymeric matrix [10, 20].

1.3.4.2 Advantages of PNPs

Using PNPs as DDS results in several pharmaceutical advantages such as:

1. Ease of manufacturing using biocompatible and non-toxic polymers,
2. Versatile technology since a wide range and type of a drug and molecules can be loaded into PNPs with high amounts of proteins, vaccine, and anticancer [11, 20-22],

3. Modulating the drug release,
4. Targeting it to a specific organ,
5. Protect it from degradation and increase its stability,
6. Improving the bioavailability and therapeutic effectiveness of the drug [11, 20, 22, 23].

PNPs can be administered by a variety of route of administration including the nasal, transdermal, intravenous, pulmonary, ocular, and orally [22].

1.3.4.3 Polymers used in PNPs

Polymers that are recommended to be used in the formulation of PNPs should be biodegradable, non-toxic, biocompatible, and not antigenic [20]. Many types of polymers are currently available for this purpose and these include natural and synthetic polymers [12].

1.3.4.3.1 Poly(lactic acid-co-glycolic acid) (PLGA)

It is one of the most commonly used polymers in PNPs formulation since it is biocompatible and nontoxic. In fact, PLGA is an FDA approved synthetic polymer which is composed of a chain of lactic and glycolic acid [24].

It is available in many molecular weights. It has an amorphous structure and glass transition temperature between 45 and 55°C which depends on the grade of PLGA [25]. It is hydrolyzed in the body to lactic and glycolic acid monomers which enter the crips cycle and they can be easily eliminated by the human body [22, 24] (Figure 1.1).

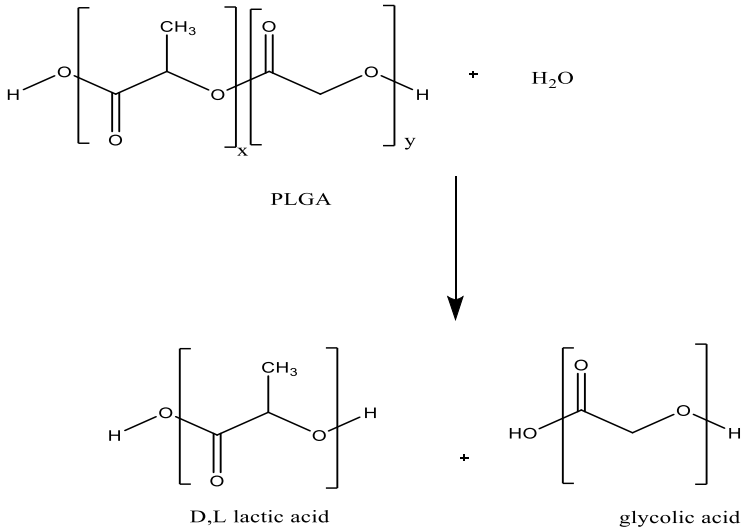

Figure 1.1: Hydrolysis of PLGA

Chemically, it can be synthesized using melt co-polymerization of the lactide and glycolide at high vacuum and constant temperature (160-190 °C) in the presence of a suitable catalyst. After that, the PLGA is purified by dissolving it in chloroform followed by precipitation using methanol [26].

PLGA polymers are soluble in many organic solvents such as acetone, ethyl acetate, dichloromethane, and benzyl alcohol [25]. Different types and grades of PLGA are commercially available. These grades have different ending group (carboxylic or ester) and the molar ratio of lactic to glycolic acid. For example, PLGA may found in the molar ratio of 75:25 lactic to glycolic acid ratio respectively [26]. Accordingly, these grades have different physicochemical properties like inherent viscosity, mechanical strength, glass transition time, and other properties. In the presences of water, PLGA adsorbs the water and hydrolyze forming water-soluble fragments with carboxylic and hydroxyl group ending. This increases the rate of degradation of PLGA which produces glycolic and

lactic acid monomer [26]. Many factors affect the degradation rate of PLGA, these factors include:

i. The ratio of lactic acid to glycolic acid in the PLGA affect the degradation rate, for instance, 1:1 lactic: glycolic ratio PLGA degrades faster than 85:15 PLGA, since increasing the lactic ratio would increase the hydrophobicity of the PLGA [26].
ii. The molecular weight of PLGA could impact the functionality of this polymer since the increase in the molecular weight of PLGA would increase the time required for its degradation.
iii. The pH of the media could affect the degradation of PLGA. In fact, the acidic or basic environment could increase the rate of degradation. Therefore, acidic and alkaline drugs should also cause the same thing if they are loaded into the PLGA polymer [25, 26].

Accordingly, the release of the therapeutic agent from PLGA polymer can vary from several days to years, depending on the factors that are mentioned above which in turn increase the flexibility of the treatments [26].

1.3.4.4 PNPs Formulation

Several methods were developed for the formulation of PNPs. These methods include a dispersion of the drug in pre-formed polymer or polymerization of the monomer.

The most common methods that are used to formulate PNPs from pre-formed polymers are:

i. Emulsion-evaporation,
ii. Nano-precipitation,
iii. Dialysis,
iv. Salting out,
v. Emulsion diffusion,
vi. And spray drying [20, 27, 28].

Therefore, the selected method and used polymer are usually based on the physicochemical properties of the drug [20].

In addition, the final properties of the obtained PNPs (size, zeta-potential, and morphology) will depend on the method of the preparation, concentration, and composition of the used polymer, viscosity of the system, stabilizer, and type of the organic solvent involved [20, 28].

1.3.4.4.1 Emulsion evaporation method (EEM)

In late 1970, PNPs with a size less than 500nm loaded with bioactive compounds were produced using EEM [28, 29].

In this technique, an organic layer composed of the polymer and a suitable organic solvent (water-immiscible organic solvent like dichloromethane) is emulsified in an aqueous layer containing a suitable stabilizer. After that, the organic solvent is evaporated to produce a suspension of PNPs [20, 21].

According to drug solubility, two approaches were found: (1) single-emulsion or (ii) double emulsion.

In the single emulsion method, the hydrophobic drug and the polymer are dissolved in the organic layer and then this layer is emulsified using the

high shear mixer in the aqueous layer that contains a stabilizer in order to form O/W emulsion (Figure 1.2). On the other hand, water-soluble drugs which do not dissolve in the organic layer and therefore they escape to the bulk aqueous layer leading to poor encapsulation efficiency (EE). Therefore, water-soluble drugs should first be dissolved in the aqueous phase and emulsified with the organic layer containing the polymer and the stabilizer in order to form the W/O emulsion. This emulsion will be emulsified with bulk aqueous phase to form double emulsion (W/O/W) emulsion followed by the evaporation of the organic phase [20, 27, 28].

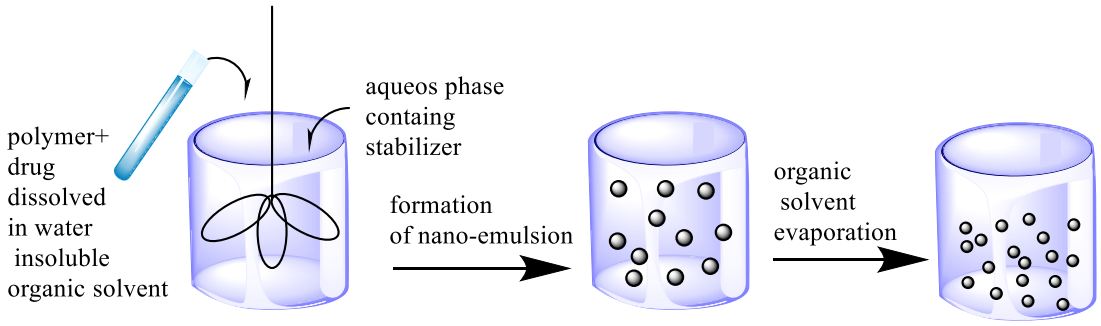

Figure 1.2: Formation of PNPs by emulsion evaporation method

1.3.4.4.2 Nano-precipitation method (NPM)

NPM is also called solvent displacement method was firstly developed by Fessi at 1989 [10]. It is usually applied to encapsulate lipophilic drugs [10, 20]. This easy and fast technique [10, 24] usually produces PNPs with a narrow size distribution, duplicate scale-up method, no energy for homogenization[10, 20], and no need for a large amount of toxic organic solvents [10].

In this method, the organic phase that contains the drug and polymer which are dissolved in a water-miscible organic solvent like acetone is dropped wise in the aqueous phase to produce PNPs. After that, the organic layer is removed by stirring at room temperature or by reducing the pressure [10, 20, 21] (Figure 1.3).

The surface properties of the obtained PNPs, such as adhesiveness, hydrophilicity, and the ability of the particle to escape from opsonization process, could be changed using coating material like polyvinyl alcohol (PVA) and polyethylene glycol (PEG) [10].

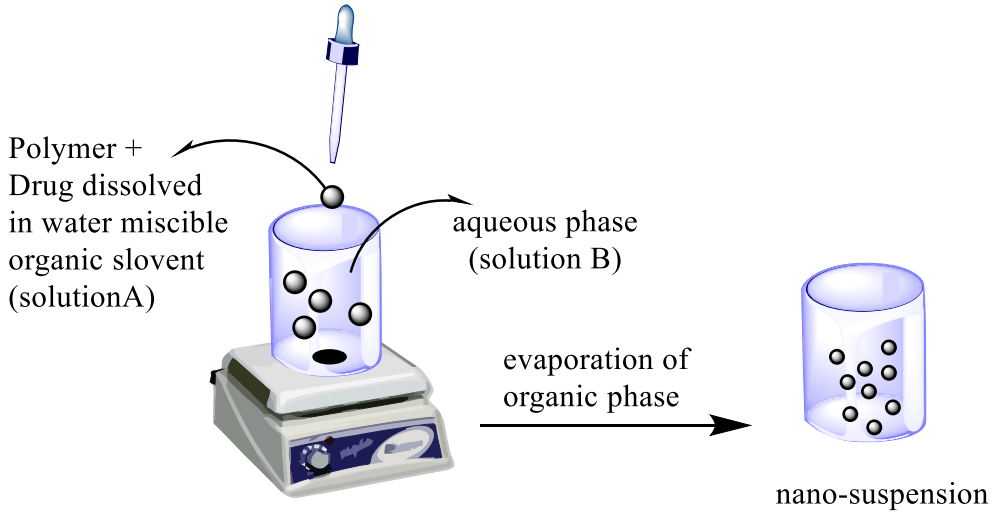

Figure 1.3: Formation of PNPs by nano-precipitation

1.3.4.4.3 Dialysis

In this method, the polymer and drug are dissolved in a water-miscible solvent. The obtained solution is placed in a dialysis bag with the specified molecular weight cut off (MCWO). Then the bag is transferred to an aqueous media. The organic phase would diffuse to the aqueous media thus reducing the solubility of the polymer which results in the formation of PNPs [20].

1.3.4.4.4 Salting out

In this technique, the polymer and the drug are dissolved in water-miscible organic solvents such as acetone or tetrahydrofuran. The organic phase is emulsified under high shear speed mixer with an aqueous phase which contains a stabilizer and high amount of salts. The high ionic strength of the aqueous phase should prevent the organic phase to diffuse into the aqueous phase. However, rapid additions of pure water to the emulsion will reduce the ionic strength and will induce the diffusion of the organic solvent into the aqueous phase resulting in the formation of PNPs after the evaporation of the organic solvent [28].

1.3.4.4.5 Emulsion diffusion method

In this method, the polymer and drug are dissolved in organic solvents that are partially miscible with water like benzyl alcohol. The obtained organic layer will be emulsified with the aqueous layer containing a stabilizer (Figure 1.4).

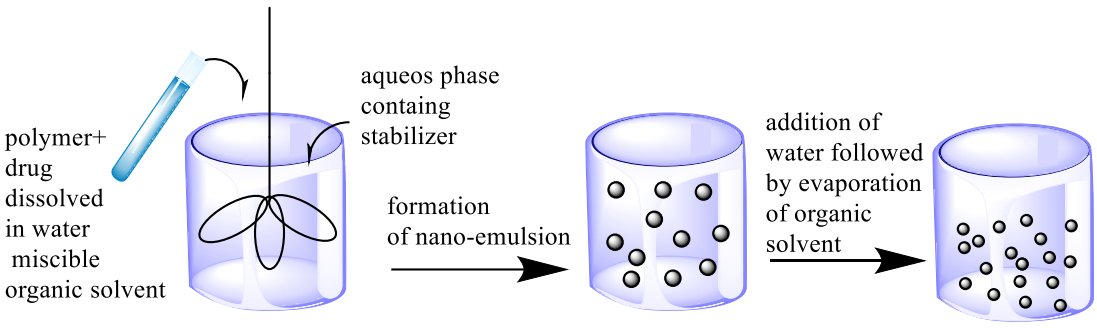

Figure 1.4: Formation of PNPs by emulsion diffusion method

The diffusion of organic solvent into the aqueous phase will trigger the formation of NPs since it is facilitated by diluting the emulsion with a large

amount of aqueous phase followed by removal of organic phase by stirring or reduce pressure [28].

The main disadvantage is large amounts of water is needed [28].

1.3.4.4.6 Spray drying

In this technique, the solid in oil dispersion or water in oil emulsion is sprayed in the presence of a steam of hot air to form NPs. Both hydrophilic and hydrophobic drugs can be encapsulated in the polymer using this method. The main disadvantage that the inner wall of spray dryer would enclose with the formed NPs [25].

1.4 Modified release dosage forms

Modified release dosage forms (MRDFs) are designed to release the active pharmaceutical ingredient (API) in a modified way in the term of time and or rate of the release of the API [30]. This can result in several advantages that including: (i) decreasing plasma drug fluctuation, (ii) decreasing the frequency of product dosing, (iii) decreasing the frequency of side effects appearance due to unwanted high level of the drug in the plasma, (iv) increasing patient drug adherence and compliance [30].

1.4.1 Types of MRDFs

According to the release pattern, MRDFs can be classified into two categories:

1.4.1.1. Delayed-release Dosage Forms (DRDFs)

These dosage forms are designed to release the major part of the API at a specific time promptly after the administration of the drug product. These products include enteric-coated dosage forms, which are usually produced to protect acid-sensitive drugs from degradation in the acidic environment of the stomach or to protect the stomach from the irritant effect of certain drugs such as diclofenac sodium [31].

1.4.1.2 Extended-release dosage form (ERDFs)

ERDFs are usually formulated to release the API over an extended period of time after the administration of the product. This results in a reduced frequency of dosing compared to corresponding immediate release dosage form [32].

1.4.1.2.1 Types of ERDFs

ERDFs are available in two types, sustained release (SR) and controlled released (CR).

1.4.1.2.1.1 SR

The release of the API from these dosage forms consists of an initial release of a part of the API sufficient to provide the initial therapeutic dose promptly after the product administration, after that a gradual release of the remaining dose over an extended period [33].

1.4.1.2.1.2 CR

These products are designed and developed to release the API at a constant rate and provide drug plasma concentration that remains constant within the time [34].

Many advantages can be achieved when patients with chronic disease rely on these products including:

i. Maintaining the therapeutic level of drug plasma at a steady state over an extended period of time and avoid drug plasma fluctuations,
ii. Reducing the side effects of the drug that associate with the highly toxic level in the drugs,
iii. Increasing patient compliance,
iv. The total cost of therapy from CR or ER formulation is lower than IR formulation so better economically to the patients and health providers [32].

1.4.2 Mechanism of drug release from these dosage forms

According to the mechanism of drug release from these dosage forms, many classes of ERDFs are available:

i. Diffusion-controlled systems

In the diffusion-controlled system, water-insoluble polymers are used to control the water hydration to the system; subsequently, the dissolved API is release from the system in a controlled manner. These products can be formulated as reservoir system, where the drug is encapsulated in the core of a polymer [33, 35].

ii. Matrix system

These systems are widely used and they are designed to release the dissolved or dispersed API in a prolonged and controlled manner. These matrices are usually composed of a well-mixed composite of one or more API with hydrophilic or hydrophobic polymers [36, 37].

iii. Erosion controlled system

Several biodegradable polymers are used to form this system in which the polymer is subjected to biodegradation. The drug release from this system is controlled by the rate of the erosion of the system and the drug release will occur at a constant rate [38].

iv. Dissolution controlled system

The drug release from the system is controlled by dissolving the coat that surrounding the drugs particles. As a result, the drug becomes available for dissolution and release. In this system, the thickness and composition of the coat control the rate of drug release [39].

v. Osmotic pump system

In this system, an osmotic agent such as sodium chloride is used to attract water from the surrounding media throughout a semi-permeable membrane that coats the drug and the osmotic agent. This generates a pressure inside the obtained capsule that pushes the API outside through a specific hole. The release is controlled by the type of osmotic agent and size of the hole [40].

vi. Ion exchange resin

In this system, the API is bound to an acidic or alkaline resin to form a salt. The release of the API will occur when exchanging with ions when it comes in contact with surrounding media [41].

1.5 Combretastatin (CA4)

Microtubules are the interesting targets for anticancer drugs. It consists of a heterodimer of an alpha and beta tubulin proteins that are polymerized into microtubules which organize the cell division, supporting cell shape, facilitating the cell transport and motility [42, 43]. Microtubules exist in the cells in an equilibrium state between polymerization and depolymerization state [42]. Any agent that disrupts the microtubules, affect morphology, division, and function of the cell would result in its death. These agents are known as microtubules distrusting agents (MDA) or microtubules targeting agents (MTA) [44]. The first identified agent is Colchicine. In fact, it was found that Colchicine binds to a β- subunit of microtubules and depolymerizes it which results in cell apoptosis and death. This process happens at a dose near the maximum tolerated dose [45]. Accordingly, many natural or synthetic agents that have a chemical structure similar to Colchicine were evaluated for their anticancer activity. This group of agents shares chemical structure that contains two aromatic rings either directly connected to each other’s or separated with one to three atoms bridge, showed some anticancer value [45]. CA4 is a natural anticancer agent that was first isolated from South African bush

willow *Combretum Caffrum* by Pettit et al. [43, 45-47]. CA4 is a Colchicine analog (Figure 1.5). It belongs to a group of drugs which known as VDA that bind to Colchicine binding site in microtubules and inhibit the polymerization. This leads to morphological changes and cell death. In addition, it has antivascular effects at a dose below the maximum tolerated dose which results in an increase in its therapeutic window and safety [42, 47, 48].

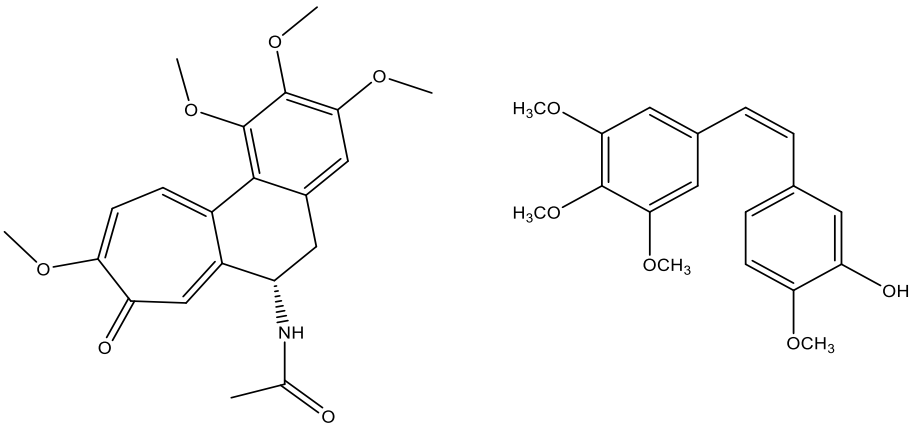

Figure 1.5: Chemical structure of Colchicine and Combretastatin (CA4)

In fact, tumor vascular endothelial cells are an interesting target for this category of chemotherapeutic agents, since it is better exposed to bloodborne chemotherapeutic agents, and no transformation in endothelial cells occurs. Accordingly, this might decrease its capacity to develop resistance to the used chemotherapeutic agents [46]. In this contest, endothelial cells are most likely affected by CA4. In fact, CA4 selectively affects tumor endothelial cells rather than normal endothelial cells [49]. Inside, CA4 inhibits angiogenesis via inhibition of vascular endothelial growth factor (VEGF) and inhibits subsequent activation of vascular

endothelial growth factor receptor-2, a receptor which mediates angiogenesis [50]. Furthermore, cancer cells depend on cellular energy production by mitochondrial oxidative phosphorylation in the form of adenosine 5′-triphosphate (ATP) to meet their demand for the neovascularization. In 2017, Lewis and co-workers conducted a study which concluded that CA4 decrease mitochondrial oxygen consumption and thus affect the ability of the tumor cells to angiogenesis [51]. Another mechanism for CA4 suggested a cleavage and activation of caspase 3 and 9 proteins, which upon activation lead to apoptosis and cell death [48]. In addition, a release of apoptosis-inducing factor (AIF) from mitochondria has been demonstrated after CA4 treatment [48]. CA4 is a water-insoluble and chemically unstable compound. In fact, it suffers from de-activation during storage due to a spontaneous transformation of cis-isomer into the inactive trans-isomer by light or heat. Accordingly, many derivatives like CA4 triphosphate (CA4P) and cis-locked chemically structures were synthesized with the aim to increase the water solubility and chemical stability of this agent [45, 48, 52-56]. CA4P is in phase III clinical trials approved for treating thyroid malignancy by Oxigene Company [52, 57, 58].

Chemically, CA4 has two aromatic rings which are connected to each other by ethylene Bridge either in cis or trans isomer (Figure 1.6). Its IUPAC name is 2-Methoxy-5-[(Z)-2-(3,4,5-trimethoxy-phenyl)-vinyl]-phenol.

From structural activity relationship (SAR) the 3,4,5 tri methoxy groups on ring A and 4 methoxy group on ring B showed a crucial role in the binding of CA4 to the Colchicine site [48, 49, 59].

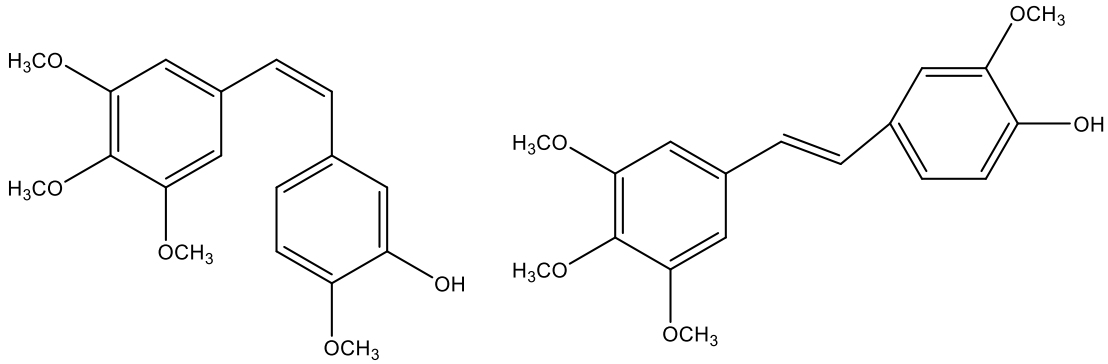

Cis COMBRETASTATIN 4 (CA4) Trans COMBRETASTATIN 4 (CA4)

Figure 1.6: Cis and trans configuration of Combretastatin CA4

To the best of our knowledge, two different approaches are available in the literature to synthesize CA4, one adopt the Witting reaction while the other uses Perkin reaction [60]. Witting reaction includes five steps giving a mixture of cis and trans CA4 with low yields of cis isomer (19%) making it not feasible for large-scale production. Another problem that faced in this method is the difficulty in the separation of the desired isomer [60]. On the other hand, the Perkin method, a stereo-selective condensation method, was developed by Letcher, selectively produced the desired cis-isomer with a higher reaction yield. In addition, the Perkin has only two steps of reaction [60]. Recently, Assali et al have successfully improved the yield through a slight modification of the Perkin method [61].

1.6 Literature review

In 2010, Yiguang Wang et al tried to develop tumor vasculature-targeted polymeric micelle for CA4. The obtained micelles were prepared using poly (ethylene glycol)-b-poly (d, l-lactide) copolymer. The study showed superior efficacy of the obtained CA4 micelles over nontargeted micelles

[62]. In the same period, Zhe Wang and et. al., had developed a tumor vascular targeted NPs [63]. These NPs were loaded with both CA4 and paclitaxel to treat tumor vascular endothelial cells. In this approach, arginine-glycin-aspartic acid (RGD) containing peptide was used as a vascular targeting agent. The loaded drug NPs system was produced firstly by charging Paclitaxel into the hydrophobic core of the PLGA polymer using NPM. After that, the hydrophobic core was coated using lipid coating in order to load CA4 in the lipid layer. In this design, the lipid layer would act as a depot for CA4 and control the release pattern of Paclitaxel from the polymer (Figure 1.7).

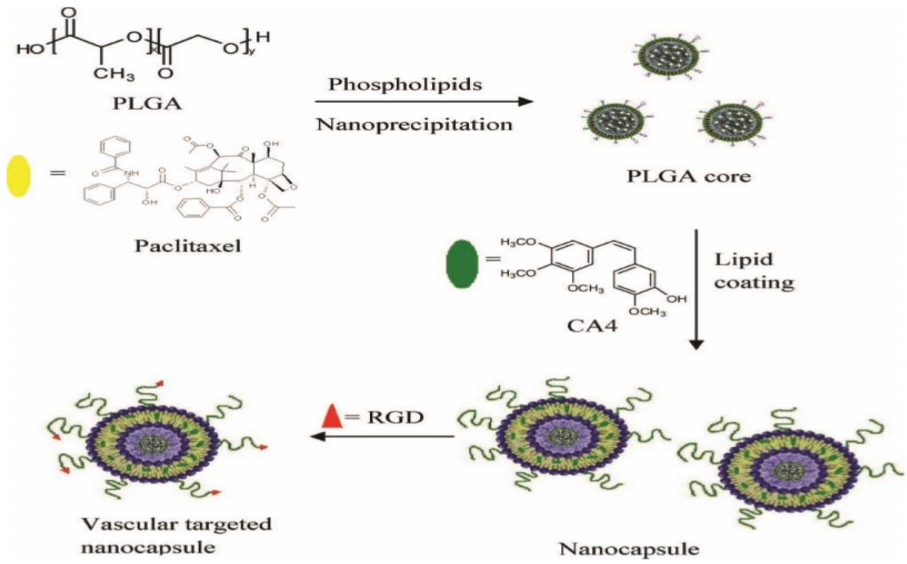

Figure 1.7: The illustration of the route of RGD-targeted nanocapsule [63]

Human umbilical vein endothelial cells (HUVECs) were used as mimetic cells to vascular endothelial tumor cells. The uptake of the NPs by these HUVECs was assessed. An efficient uptake of both drugs by HUVECs was observed and an improved potency and cytotoxicity of these drugs

were recorded [63]. Another study was conducted by Zhe wang and et al. to develop a targeted paclitaxel and CA4 PLGA NPs. In this study, the authors tried to increase the loading efficiency of the developed NPs by using the EEM. After that, the obtained capsules were conjugated with RGD as a targeting ligand peptide. The encapsulation efficiency% (EE %) ranged from 53% to 57% for CA4 and 63% to 65% for paclitaxel (Figure 1.8).

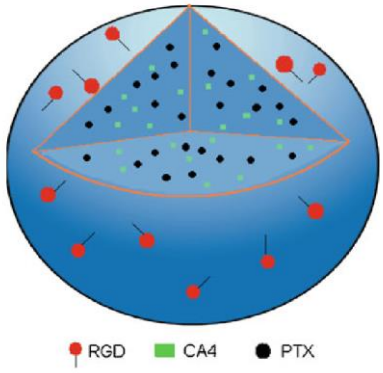

Figure1.8: A drawing structure of CA4 PTX targeted PLGA nanoparticle [64]

The paclitaxel-CA4 PLGA NP showed significant anticancer and anti-angiogenesis activity on mouse model [64]. Another study has been conducted by Wang, Y and et al. using a combination of CA4 and methotrexate (MTX) NPs, using a pH-sensitive model, against hepatocellular carcinoma(HCC) [65]. In this study, the N-urocanyl pullulan (URPA) was synthesized and reacted with MTX. The resultant spherical NPs had a size range between 200 to 250 nm [65]. Under acidic conditions, the URPA group becomes protonated and bearing a positive charge, which highly improved the hydrophilic properties of the obtained NPs and an

increase in the release of CA4 in the tumor cells as their pH is more acidic than the normal healthy tissue was observed [65] (Figure 1.9).

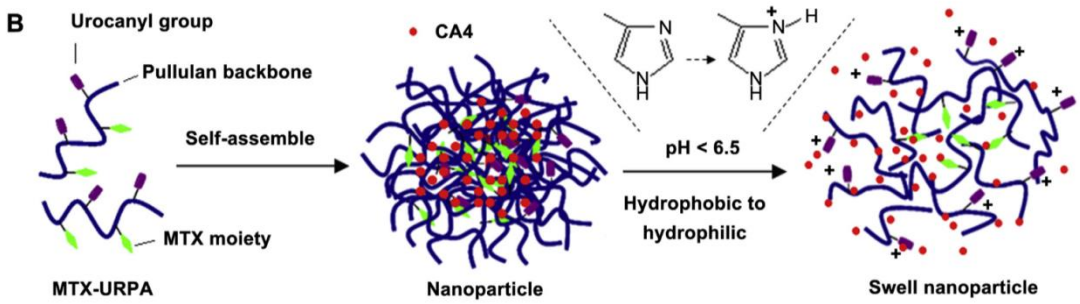

Figure1.9: Demonstration of formation of CA4/MTX-URPA NPs [65]

In addition, *in vivo*, using tumor-bearing mice was conducted to assess the cytotoxicity of the obtained CA4/MTX-URPA NPs. A significant improvement in the tumor regression was observed at the end of the treatment [65]. In 2016, Burcu Sumer Bolu and co-workers covalently linked CA4 to a tri-block dendron with a polyester ending. The obtained NPs would accumulate in tumor mass and start the release of the CA4 into the tumor tissue (Figure 1.10).

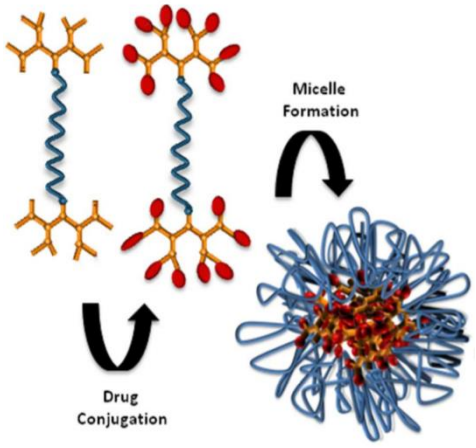

Figure 1.10: Scheme of formation of CA4 flower-like micelles[66]

A significant anti-angiogenesis effect against HUVECs of the obtained CA4 conjugated to a tri-block dendron was recorded [66]. In 2017, Yang

Ou and co-workers developed micelle-like CA4 NPs. In this study, the CA4 was chemically bonded, through esterification reaction to pegylated poly (glutamic acid) copolymer (PLG-g-PEG) in order to produce CA4-PL micelles. In fact, spherical micelles-like NPs, with an average particle size around 100 nm, were obtained. These NPs release CA4 in the tumor cells due to the higher acidity of the tumor cells than blood. In fact, this would result in an increase in the circulation time and CA4 stability which in turn results in an improvement in the therapeutic outcome of CA4 [57] (figure 1.11).

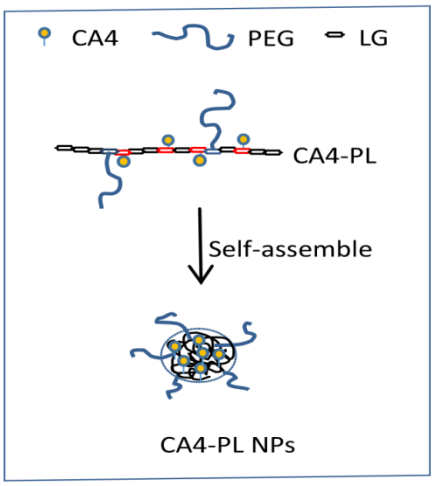

Figure 1.11: Scheme rout for CA4-PL NPs self-assembly [57]

In 2018, the study was performed by Assali M and co-workers to load CA4 into functionalized carbon nano-tube to produce an SWCNT-CA4 system in order to increase the solubility of CA4 and targeting toward cancer cells. The study indicates that SWCNT-CA4 had significant necrotic effects on HeLa cells, making it superior as a therapeutic agent than free CA4 in the treatment of cancer [67].

1.7 The objective of this study and working plan

1.7.1 Objectives of the study

The aim of this study is to encapsulate the CA4 into PLGA polymer to produce PNPs (spherical, around 200 nm in size, with zeta-potential between -20 to -40 mV) in order to increase the CA4 targeting towards tumor, and consequently decreases the side effects of CA4, as well as increases the potency and half-life of the drug, and decreases the need for multiple dosing that result in increasing the patient compliance.

1.7.2 Working Plan

1.7.2.1 Synthesis and Characterization of CA4.

1.7.2.2 Preparation and optimization of PLGA NPs.

1.7.2.3 Loading CA4 to PLGA NPs.

1.7.2.4 Calculation of encapsulation efficiency (EE%) and Drug Loading % (DL%).

1.7.2.5 Assessment of particle size and zeta-potential of the obtained NPs using Zeta sizer.

1.7.2.6 Characterization of the Morphology of obtained NPs using transmission electron microscope (TEM).

1.7.2.7 Assessment of the kinetic *in vitro* release of CA4 from PLGA NPs.

1.7.2.8 Assessment the *in vitro* cytotoxicity of CA4 NPs.

Chapter Two

Experimental Part

Materials & Methods

2.1 Materials

All materials used in the synthesis CA4 and NPs were of analytical grades. 2-(3,4,5- trimethoxyphenyl) acetic acid, 3-hydroxy-4-methoxybenzalde, and quinoline were purchased from Alfa Aesar Company (England). Acetic anhydride and copper were purchased from Sigma-Aldrich (USA). Hexane and ethyl acetate from Frutarom.

In order to purify the obtained reaction products, column chromatography using silica gel (pore size 60 Å, 40-63 µm particle size, 230-400 mesh particle size) was used. This silica was purchased from Sigma-Aldrich Company (USA). The reactions were monitored using TLC (DC-Fertigfolien Alugeram®Silg/Uv254, Macherey Nagel Company (Germany). For NPs synthesis PLGA 502H was purchased from Sigma-Aldrich (Germany), acetone from Fisher chemical (UK), dichloromethane from AZ Chem company (China), PVA 99% hydrolyzed powder with MWT 89000-98000 from Sigma-Aldrich (USA), methanol from Romil pure chemistry, acetonitrile from Scharlau (Spain).

Phosphotungstic acid solution 10% W/V was purchased from Sigma Aldrich (Switzerland) that was used in the characterization of NPs.

Dialysis tubing cellulose membrane, with flat width 43mm MWCO 14000 kDa, was used to conduct the *in vitro* release (IVR) study. This tube was purchased from Sigma-Aldrich Company (USA).

Materials that are used in the preparation of buffer solutions are sodium dihydrogen phosphate anhydrous from AZ Chem for chemical (India), potassium dihydrogen phosphate from AZ Chem for chemicals (China), sodium phosphate dibasic dihydrate from Sigma-Aldrich (Germany), potassium chloride from Xiong chemical industry (China), NaCl from AZ Chem for chemical (Germany).

For tissue culture, DMEM growth culture media and penicillin-streptomycin solution 100X were purchased from Euro-clone, Italy. Phosphate buffer saline 1X from Eurobio, France.

Trypsin EDTA 10X solution from Santa Ana, California, and dimethyl sulfoxide (DMSO) from Scharlab, spain, while Thiazolyl Blue Tetrazolium Bromide from Sigma-Aldrich, USA. All the materials that were used for *in vitro* cytotoxicity assay are for cell tissue culture use grade.

2.2 Equipment and tools

Tools and equipments used in this study are listed in table 2.1.

Table 2.1: List of tools and equipment used in the study

Equipment	Source/model
Centrifuge	Germany, model number Z216M
Digital multi stirrer	Italy, model number F203A0179
Light dynamic scattering	UK, Zetasizer Nano-ZS Malvern, model number ZEN3600
Paddle sonicator	Germany, model number UP200Ht
plate reader	USA ,BioTek
Shaker incubator	Korea, model number LSI-3016A
Transition electron microscope	Netherlands, Morgagni 286 transmission microscope
UV-vis spectrophotometer	USA, Evolution 220, 840-210600

2.3 Methods

2.3.1 Synthesis of CA4

CA4 was synthesized according to the method published by Xiao et al with some modification as reported by Assali et al [61, 68].

Precisely, 4.33ml (46.41 mmol) of acetic anhydride and 2.22ml (15.91 mmol) of triethylamine was added to 3g (13.26 mmol) of 3,4,5-trimethoxyphenyl acetate and 2.421g (15.91 mmol) of 3-hydroxy-4-methoxy benzaldehyde. The reaction was carried out using 50ml of DCM and heated to 110°C under reflux for 4 hr. The reaction was cooled to room temperature (RT), acidified using 2M HCl and kept overnight in an ice bath. The day after, a dark brown precipitate was found. The supernatant was discarded and 30ml of 10% NaOH solution was added to dissolve the

brown precipitate and washed using 100ml ethyl acetate. After that, the cinnamic acid derivative was precipitated using 2M HCl. The product was filtrated and dried. Then the dried product was recrystallized using ethyl acetate.

4.66g of copper and 3.3g of cinnamic acid derivative were added to 15ml quinoline under argon conditions and magnetic stirring for 3hr at 200 °C. After that, the reaction was cooled to RT, the copper was filtered away and CA4 was extracted using 100 ml ethyl acetate and washed using 50ml 2M HCl solution, then the organic layer was cleaned using 50ml of saturated NaCl solution. The cleaned organic phase was dried using anhydrous Na_2SO4 to obtain a viscous brown liquid that contains the CA4 product. CA4 was purified using flash column chromatography with a mobile phase composed of hexane: ethyl acetate (7:3). Further purification by recrystallization was carried out by ethyl acetate: petroleum ether (1:9) to obtain white powder CA4.

2.3.2 Calibration curve of CA4

A CA4 Calibration curve was constructed in order to calculate the amount of CA4 loaded in PLGA NPs. For this purpose, 50 µg/ml concentration of CA4 in acetonitrile was prepared as a stock solution in which the lambda max was determined by UV-vis scanning (300nm). After that, a series concentration of CA4 (50, 40, 30, 21, 10.5, and 5.25 µg/ml) were prepared by a serial dilution from the stock solution using acetonitrile. The

absorbances of solutions were measured at λmax 300nm using UV-vis spectrophotometer.

Another calibration curve was made for calculating the released amount of CA4 in *in-vitro* release method which was performed in phosphate buffer saline in which 1% SLS was added to it. For this purpose 50 µg/1ml concentration of CA4 in 1% SLS in PBS (PH=7.4) was prepared as a stock solution in which the lambda max was determined by UV-vis scanning (304nm). After that, a series concentration of CA4 (50, 40, 28, 19.6, 11.76, 5.88 and 2.94 µg/ml) were prepared by a serial dilution from the stock solution using 1% SLS in PBS (PH=7.4). Then, the concentration of CA4 in the solution was measured by UV-vis spectrophotometer at 304nm.

2.3.3 Preparation of CA4 loaded PLGA PNPs

Several trials were conducted to prepare PLGA NPs, using different PLGA grades (502H and 504H) and changing others under different formulation conditions. In addition, both nano-precipitation and emulsion evaporation methods were approached to prepare CA4 loaded PLGA NPs.

2.3.3.1 Nano-precipitation method (NPM)

A solution of 50mg or 100mg ± 0.1mg of PLGA and 1mg± 1µg of CA4 in 2ml acetone was added drop wise to 5ml phosphate buffer (PH=7.4) under magnetic stirring at 400 RPM, then the mixture was kept overnight under magnetic stirring at 400 RPM until complete evaporation of acetone. The CA4 loaded PLGA NPs were collected by centrifugation at 15000 RPM

for about 10 min. The free CA4 was removed by washing the NPs with methanol and the NPs were collect by centrifugation. Blank PLGA NPs were prepared using the same steps but without the CA4 drug. All the formulae above were made in triplicate (Table 2.2).

Table 2.2: Formulation trials of a nano-precipitation method

Component	Trial code					
	A1	A2	A3	A4	A5	A6
PLGA 502H (mg)	-	-	50	100	50	100
PLGA 504H (mg)	50	50	-	-	-	-
CA4 (mg)	-	1	-	-	1	1
Acetone (ml)	2	2	2	2	2	2
Phosphate buffer (PH=7.4) (ml)	5	5	5	5	5	5

2.3.3.2 Emulsion evaporation method (EEM)

In this method, PLGA and CA4 were dissolved in DCM and emulsified with PVA1% using paddle sonicator at an energy output of 50W for 30 seconds under ice bath. Then, the O/W emulsion was kept under magnetic stirring at 400 RPM for 8hr until complete evaporation of DCM. The CA4 loaded PLGA was collected by centrifugation at 15000 RPM for 10 min and the free CA4 was removed by washing the NPs with methanol and centrifugation to collect the NPs for further characterization. Blank PLGA NPs were prepared by the same method but without the CA4 drug. All the formulation trials were made in triplicates (Table 2.3).

Table 2.3 : Formulation trials of an emulsion evaporation method

Component	Trial code									
	A7	A8	A9	A10	A11	A12	A13	A14	A15	A16
PLGA 502H (mg)	-	-	50	100	50	50	100	100	100	100
PLGA 504H (mg)	50	50	-	-	-	-	-	-	-	-
CA4 (mg)	-	1	-	-	1	2	1	2	4	8
PVA (mg)	50	50	50	50	50	50	50	50	50	50
DCM (ml)	1	1	1	1	1	1	1	1	1	1
DDIW (ml)	5	5	5	5	5	5	5	5	5	5

2.3.4 Characterization of CA4 loaded PLGA NPs

2.3.4.1 Particle Size and zeta-potential

The intense mean diameter size and zeta-potential of CA4 loaded PLGA NPs and the blank NPs were measured using light dynamic scattering (DLS).

2.3.4.2 Encapsulation efficiency (EE %) and Drug loading (DL %)

EE% and DL% of CA4 loaded PLGA NPs were calculated by dissolving determined quantities of CA4 loaded PLGA NPs in 2ml ACN and lifted under magnetic stirring for 3 hrs for complete dissolving of the NPs, and the CA4 content in the solution was measured using UV-vis spectrophotometer at 300nm. EE% and DL% were calculated according to equation 1 and 2.

$$\%EE = \frac{Amount\ of\ loaded\ CA4\ (\mu g)}{\text{amount of initial weight of CA4 } (\mu g)} x100 \qquad eq.1$$

$$\%DL = \frac{Amount\ of\ loaded\ CA4\ (\mu g)}{weight\ of\ CA4\ loaded\ PLGA\ NPs\ (\mu g)} x100 \qquad eq.2$$

2.3.4.3 Morphology of CA4 loaded PLGA NPs and blank NPs

The shape and morphology of CA4 loaded PLGA NPs and the blank formula was carried out using transition electron microscope (TEM). Two samples were prepared, CA4 loaded PLGA NPs (formula A14) and same formula but without CA4 (A10). For this purpose, one drop was added to the carbon-coated copper grid, forming a thin liquid film.

The negative staining with phosphotungstic acid was used to increase the contrast of the images.

2.3.4.4 Mathematical Calculation

The 2^2 factorial designs were constructed to investigate the impact of the concentration PLGA and CA4 on the particle size, zeta-potential, and EE% of the obtained PNPs. The two independent variables are PLGA as (X1) and CA4 as (X2). Each independent variable had 2 levels which were coded as –1 and +1. The coded values of independent variables were given to the software as shown in Table 3.3. The four runs in design matrix of 2^2 full factorial designs are set up by randomization. A multiple regression, first-degree model was used to express the response as a function of the selected factors. Design-Expert version 8.0.7.1 was applied for performing the experimental design and the data analysis [69].

2.3.4.5 *In-vitro* release study of CA4 loaded PLGA NPs

IVR of CA4 loaded PLGA NPs was performed. For this purpose, 85mg of CA4 loaded PLGA NPs was used from formula A14. The NPs were suspended in 2ml PBS (PH=7.4) in which SLS1% was added to it and placed into a dialysis membrane bag, then the dialysis bag was immersed in 14ml of the previous medium (SLS1% in PBS, PH=7.4) and kept under 100 RPM shaking at 37˚C using shaker incubator. An aliquot (1ml) was withdrawn from the dissolution medium and replaced with the same amount of fresh medium to maintain the sink condition. The sample was centrifuged at 6000 RPM for 15 min and the amount of CA4 released was measured using UV-vis spectrometer at 304 nm. The same procedure was carried out also on the blank formula (A10). The process was made in triplicate. The IVR data were analyzed using DDSolver program (version 1.0) to describe the release behavior of the CA4 from PLGA NPs using several kinetic release models such as zero-order, first order, Higuchi, Peppas, and Korsmeyer, Hixon-crowell, and others (Table 3.4).

2.3.4.6 Stability of CA4 loaded PLGA NPs

The stability of CA4-loaded PLGA NPs (formula A14) was determined by measuring the variation in the particle size of NPs as a function of time at 4 and 25˚C for 4 days. The particle size was determined using DLS device.

2.3.5 *In-vitro* cytotoxicity

The anticancer activities of free CA4 in DMSO, free NPs (PLGA NPs without CA4), and charged NPs (CA4 loaded PLGA NPs) in phosphate buffer were assessed against two lines of cancer cells, Caco-2 and HeLa.

2.3.5.1 Cell culture

Caco-2 and HeLa cells were grown using 15-cm^2 plastic culture plates. The culture growth medium (CGM) was composed of DMEM medium. 10% fetal bovine serum (FBS), L-glutamine, and penicillin/streptomycin were used as a supplement for the medium. Cells were incubated in the above prepared medium and kept at 37°C in a humidified atmosphere enriched with 5% CO_2. For sub-culturing, the obtained CGM was suctioned from the culture plates. After that, the cells were washed using 7ml of Ca^{2+}-free PBS. Then, 1 ml of trypsin was added to the cells and were incubated for 5 minutes under the above-stated growth conditions. After that, 3ml of CGM were added under gentle mixing to inactivate trypsin, and subsequently, the cell suspension was placed into 96-well plate in appropriate cell number and lifted for 24 hrs to allow appropriate adherence of the cells to the plates.

2.3.5.2 Cell viability test

Different concentrations of free CA4, free NPs, and charged NPs were added to cancer cell lines (Caco-2 or HeLa) and incubated under the above-mentioned conditions. Reading was recorded at specific interval

times, 24 and 48 hrs. Then, 20 µl of MTT solutions was added to each well followed by an incubation period of 3hrs, then the media were removed and 200 µl of DMSO was added to dissolve the crystal and the absorbance was recorded at 530 and 670 nm wavelength using plate reader.

Chapter Three

Results and discussion

3.1 Synthesis and formulation of CA4

CA4 was successfully synthesized and purified giving a yield around 36.36% of a white powder. In addition, solubility analysis was conducted on CA4 in order to select the most suitable solvent to formulate the drug and to construct a suitable and simple spectrophotometric method for the analysis and quantification of a CA4. For this purpose, a calibration curve of CA4 has been constructed. Moreover, H-NMR spectrum was also conducted to prove its identity and purity of the product.

3.2 Calibration curve of CA4

Calibration curve of CA4 in acetonitrile was constructed, with R^2 equal to 0.999, in order to calculate the loaded amount of loaded CA4 in PLGA NPs (Table 5.1). The observed maximum UV absorption of CA4 was at 300nm (Figure 3.1).

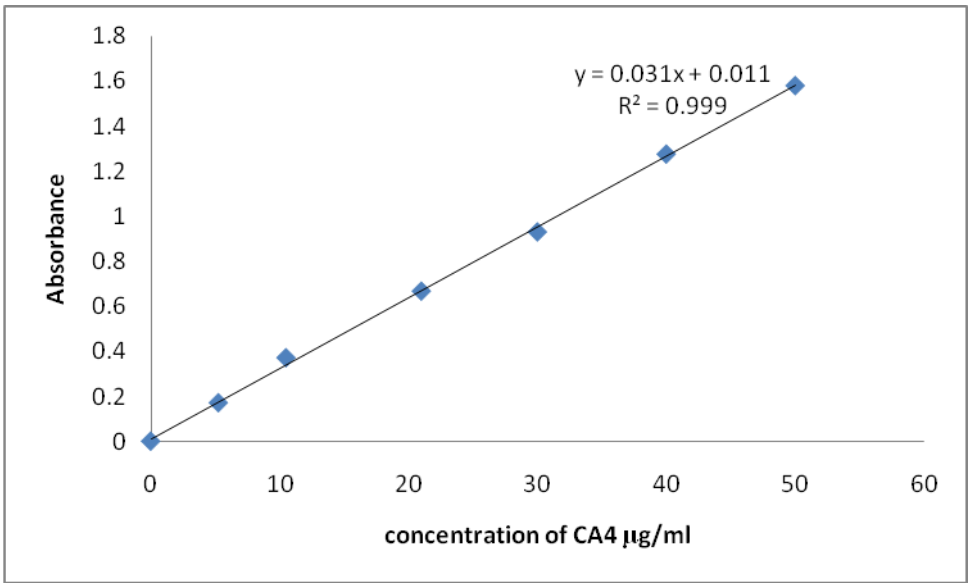

Figure 3.1: Absorbance versus concentration Calibration curve of CA4 in acetonitrile at 300nm

Calibration curve of CA4 in PBS with 1% SLS was constructed, with R^2 equal to 0.999, in order to calculate the released amount of CA4 from PLGA NPs in 1% SLS in PBS (Table 5.2). The observed maximum UV absorption of CA4 was at 304nm (Figure 3.2).

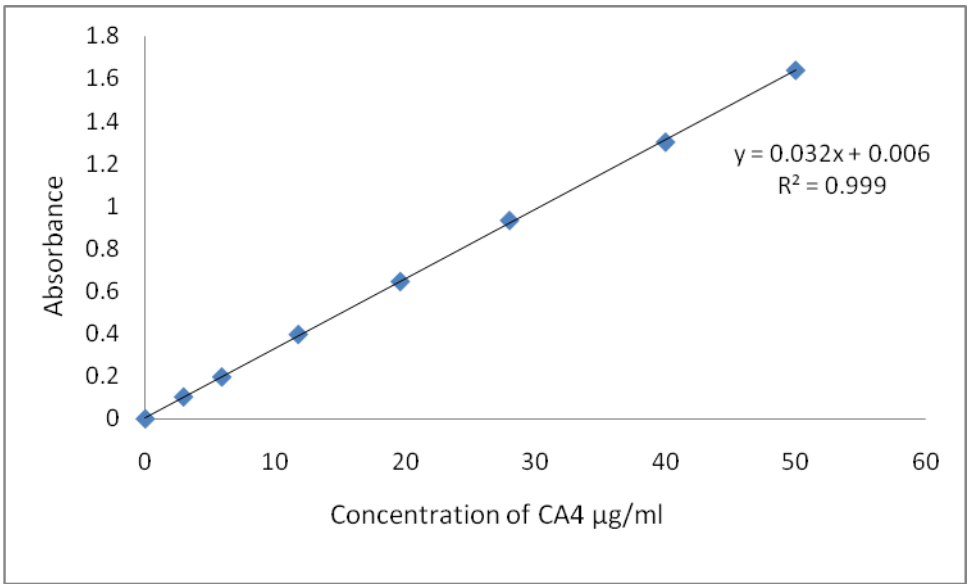

Figure 3.2: Absorbance versus concentration Calibration curve of CA4 in PBS PH=7.4 containing 1% SLS at 304nm

3.3 NPs formulation

After successful synthesis and purification of CA4, many attempts were conducted to encapsulate it within PLGA NPs. For this purpose, two formulation techniques, emulsion evaporation, and nano-precipitation were approached with the attempt to find the best one in terms of EE%, shape, size, and release profile. In addition, we benefit from the biodegradable characteristic of PLGA polymer in synthesizing anticancer CA4 loaded PLGA NPs as a controlled drug delivery system [71]. Here in, several parameters were controlled and varied in order to obtain the best condition for the optimum formulation with highest EE% and small particle size. These parameters include the method of preparation of NPs, amount and type of the used polymer, and amount of CA4 used (Table 3.1 and 3.2).

3.3.1 Effect of PLGA grade

Two types of PLGA polymer (PLGA 504H and PLGA 502H) were tried to produce NPs. Despite the used concentration, PLGA 504H gave sticky aggregates when NPM was used. However, this inconvenient disappeared when EEM was used. Accordingly, this grade was initially selected to formulate our NPs. Unfortunately; it gave UV interferences with CA4 absorption during the EE% and DL% determination. Therefore, PLGA 502H grade was used. In fact, this last one gave satisfactory results since no sticking or analytical interferences with the drug were registered.

3.3.2 Effect of the used method

3.3.2.1 Nano-precipitation method

Suitable small blank and CA4 loaded NPs were successfully produced (Table 3.1). Unfortunately, EE% was unsatisfactory, therefore, another method, EEM, was tried (Table 3.2).

Table 3.1: Formulation variables and observed quality of NP by nano-precipitation method

Components	Trail code			
	A3	A4	A5	A6
PLGA 502H (mg)	50	100	50	100
CA4 (mg)	-	-	1	1
Acetone (ml)	2	2	2	2
Phosphate buffer (PH=7.4) (ml)	5	5	5	5
Particle size (nm) ± SD	118.53 ± 1.86	192.93 ±4.41	116.93 ± 0.91	198.37 ± 0.01
PDI ± SD	0.147 ±0.019	0.162 ± 0.021	0.155 ± 0.007	0.164 ± 0.008
Z-potential (mV) ± SD	-68.60 ± 0.70	-75.87 ±0.67	-68.87 ± 0.08	-77.63 ±0.67
EE% ± SD	-	-	31.24% ±3.20	32.211% ±2.722
DL% ± SD	-	-	0.61% ±0.084	0.406% ±0.021

3.3.2.2 Emulsion evaporation method

The EEM was able to produce a higher amount of EE% than nano-precipitation method. Accordingly, this method was adopted as a master preparation method to produce NPs. However, additional trials were conducted to improve the quality of the obtained NPs such as EE%, zeta-potential, and particle size (Table 3.2).

Table 3.2: Formulation variables and observed quality of NP by emulsion evaporation method

Component	Trial code							
	A9	A10	A11	A12	A13	A14	A15	A16
PLGA 502H (mg)	50	100	50	50	100	100	100	100
CA4 (mg)	-	-	1	2	1	2	4	8
PVA (mg)	50	50	50	50	50	50	50	50
DCM (ml)	1	1	1	1	1	1	1	1
DDIW (ml)	5	5	5	5	5	5	5	5
Particle size (nm) ± SD	196.00 ± 3.73	207.70 ± 0.44	193.00 ± 2.15	181.87 ±1.81	206.93 ± 3.49	203.25 ± 0.49	205.13 ± 3.35	200.00 ± 0.14
PDI ± SD	0.141±0.009	0.140± 0.009	0.120± 0.018	0.098± 0.009	0.141± 0.006	0.16± 0.028	0.146± 0.021	0.117± 0.016
Z-potential (mv) ± SD	-28.36 ± 1.42	-36.77 ± 0.31	-24.73 ± 0.38	-32.93 ±1.08	-37.10 ± 1.13	-38.50 ± 1.05	-34.43 ± 2.14	-33.66 ± 0.32
EE% ± SD	-	-	40.92% ± 3.05	28.87% ±2.16	46.00% ± 0.03	50.84% ± 6.24	41.55% ± 0.53	36.15% ± 4.45
DL% ± SD	-	-	0.93% ± 0.06	1.60% ±1.40	0.51% ± 0.04	1.13% ± 0.09	1.86% ± 0.17	3.43% ± 0.46

In these trials, all components were kept at the same level of concentration, except for PLGA which was used in two concentration levels, high and low (Table 3.2). In addition, growing concentrations of CA4 were also used and the observed responses in term of EE%, DL%, zeta-potential, and average particle size were recorded (Table 3.2). As shown in Table 3.2, in trials A11 and A13, all components were kept at the same level of concentration except for the level of PLGA which was duplicated (50 and 100 mg). It can be observed that a better EE% was observed at the higher PLGA concentration (100 mg). Moreover, further attempts were conducted to increase the EE% of CA4. This was carried out by increasing the concentration of CA4. As can be shown in table 3.2, an improvement of the EE% was observed at a CA4 concentration equal to 2 mg. However, this increase cannot be considered as a general trend or pattern, since the EE% was almost the same at higher CA4 concentrations (Table 3.2). Precisely, when the amount of CA4 was increased from 1mg to 2mg an increase in the EE% was observed (46.00% ± 0.03 to 50.84% ± 6.24 respectively). However, increasing the amount of CA4 from 4 to 8 mg resulted in a decrease in EE% (41.55% ± 0.53 and 36.15% ± 4.45 respectively) despite increasing in DL%. This may be due to the constant size of the obtained NPs and accordingly may affect the maximum amount of encapsulated drug.

3.3.3 Statistical assessment

For this purpose, 2^2 factorial designs were adopted to assess the statistical impact of the concentrations of PLGA and CA4 on EE%, zeta-potential, and particle size of the obtained NPs (Table 3.3).

Table 3.3: 2^2 factorial design matrix

Run 1	Kind of variable		Response		
	X1 (PLGA)	X2(CA4)	EE%	Particle size	Zeta-potential
1	-1	+1	28.9	181.9	-32.9
2	+1	-1	46.0	206.9	-37.1
3	+1	+1	50.8	203.3	-38.5
4	-1	-1	40.9	193.0	-24.7

The results of this factorial design showed the positive effect of the concentration of PLGA but not significant effect on both EE% and particle size (p-value was higher than 0.05). Vice versa, the concentration of CA4 had negative but not significant effect on both particle size and EE% (p-value higher than 0.05). Concerning zeta-potential, both PLGA and CA4 had negative but not significant effect as shown in half–normal plot (Figure 3.3).

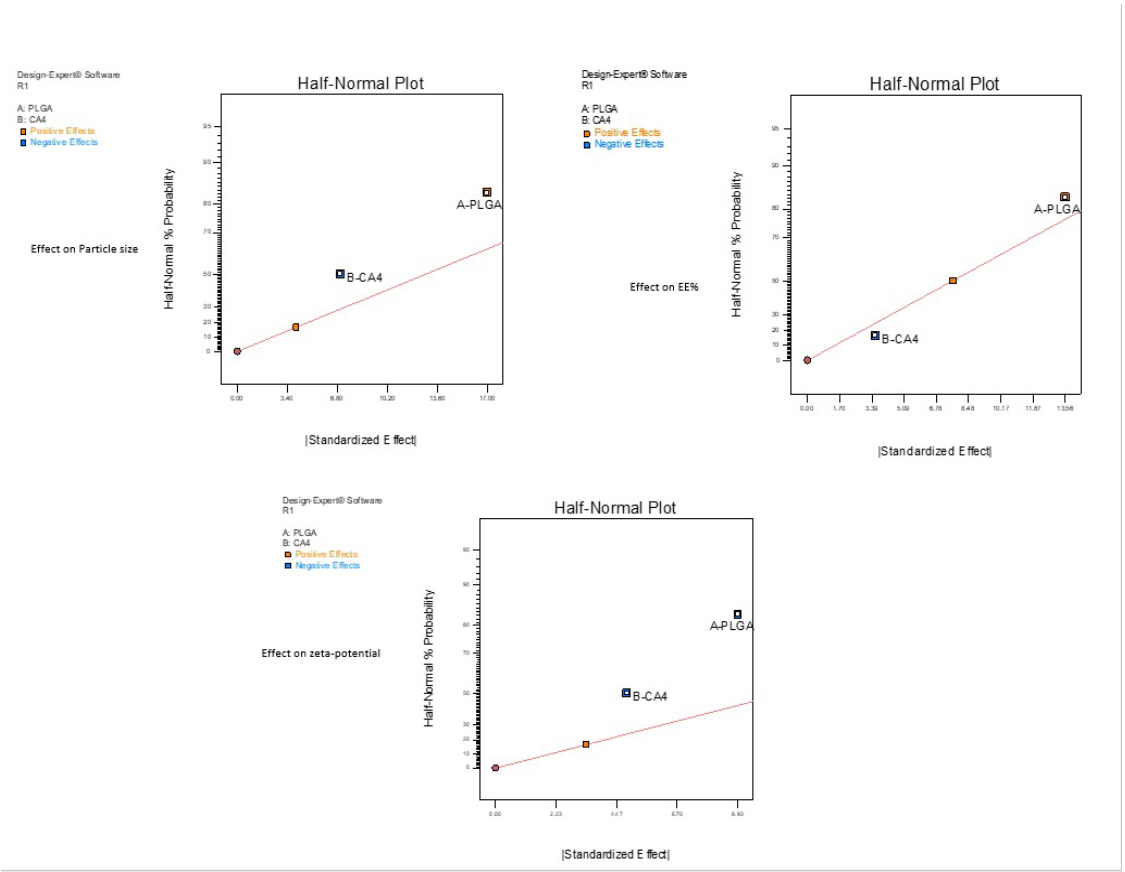

Figure 3.3: Normal probability plot of the effect of PLGA and CA4 concentration on the final characteristics of obtained NPs

Accordingly, formula A14 was adopted to produce the desired CA4 loaded PLGA NPs.

3.3.4 Particle size, Zeta-potential, and surface characteristics analysis

The particle size and surface characteristics of the obtained NPs were investigated since they are considered as a primary feature that may influence the bioavailability of encapsulated anticancer drug to tumor tissue. In fact, recent *in vitro* and animal model studies were conducted by Yao J, and et al. These studies have demonstrated the importance of NPs sizes lower than 200 nm to achieve longer systemic circulation time, lower cytotoxicity, greater stability, and favorable uptake by the enhanced

permeability and retention effect [72-79]. In addition, in 2016, Saha C et al. Found that relatively larger sizes (<500 nm) NPs are subjected to systemic lavage and have demonstrated the need for suitable modifications of their surface in order to potentially evade mononuclear phagocytic system (MPS) recognition [80].

As can be shown in Table 3.2, the amount of PLGA slightly increased the size of NPs. In fact, using the same amount of CA4 (1mg) and changing the level of PLGA from 50 mg to 100 mg, an increase in particle size from 193.00 ± 2.15 to 206.93 ± 3.49 nm was observed. This can be explained by the increase in the amount of PLGA, which results in an increase in the viscosity of the emulsion, so the sonicator becomes less effective in breaking the particles into smaller ones. In fact, this hypothesis was also confirmed by other studies such as Sharm and et al., who assessed the effect of process and formulation variables on paclitaxel loaded PLGA NPs [81]. In addition, Bohrey and co-workers also noticed an increase in the mean particle size of diazepam PLGA NPs when the amount of PLGA was increased [82]. Moreover, this increase in particle size was noticed in our study (p-value less than 0.05) when the amount of PLGA was increased from 50 to 100 mg using NPM.

Concerning the surface morphology of the obtained NPs, both drug loaded and blank PLGA NPs were assessed using TEM. The shape of the particles that were measured revealed that they have almost spherical in shape with the relatively smooth surface with minor fluctuations in the obtained sizes [83] (Figure 3.4).

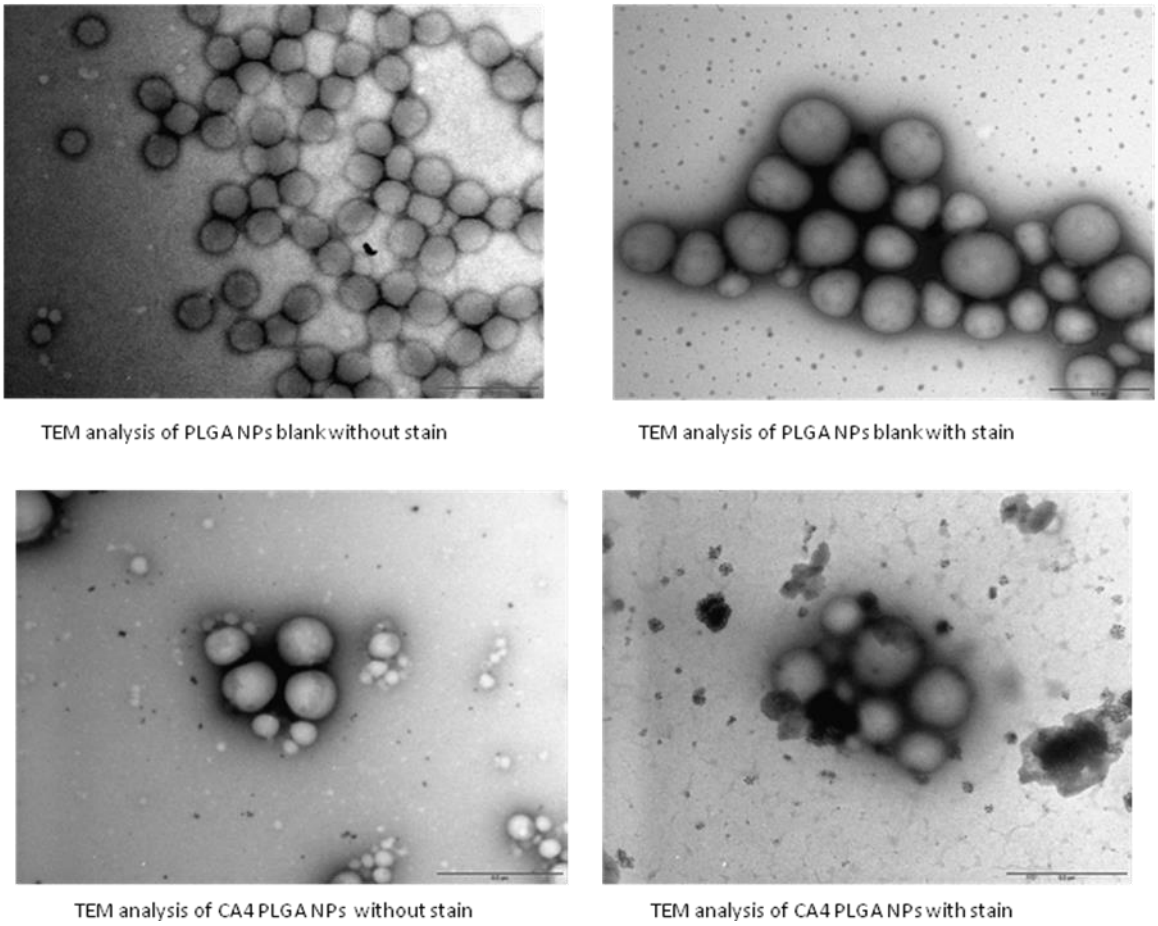

Figure 3.4: Transmission electron images of CA4 PLGA and blank PLGA NPs*Phosphotungstic acid was used as a contrasting agent

Regarding the surface charge, a higher negative zeta-potential was noticed when the amount of PLGA was increased, from -24.73 ± 0.38 to -37.10 ± 1.13 mV (table 3.2). In fact, the used PLGA (502H) encompasses a carboxylic ending group, so the increase of the amount of used PLGA would result in an increase in the negative charge at the surface of the obtained NPs. However, the obtained negative zeta-potential remained within the desired balance to achieve cellular uptake and lower *in vivo* cytotoxicity. Recently, several studies reported that the type and value of zeta-potential greatly regulate the cellular interaction of NPs. In fact,

cationic NPs demonstrated higher cellular uptake than anionic NPs [77-80]. On the other hand, an increase *in vivo* cytotoxicity was observed in the case of positive surface charged PNPs. Therefore, suitable surface modification to shield cationic groups using polyethylene glycol (PEG) has demonstrated a reduction in the cytotoxic effect caused by the cationic charges [16]. In addition, it was demonstrated that NPs with a low anionic charge (−20 mV to −40 mV) would be ideal candidates for *in vivo* application since they can strike a balance between charge related cytotoxicity and cellular uptake [71, 75]. Therefore, the obtained negative zeta-potential is in agreement with our target and no need for surface modification of the obtained NPs.

3.3.5 *In vitro* release of CA4 from PLGA NPs

Figure 3.5 shows the time-dependent CA4 release from PLGA NPs (formula A14) in PBS PH= 7.4 in which SLS 1% was added to it at 37˚C.

The release of CA4 from PLGA NPs was studied for 17 days. CA4 released from PLGA NPs showed SR manner. In fact, it takes 17 days to release 87% of CA4 capsulated (Table 5.3).

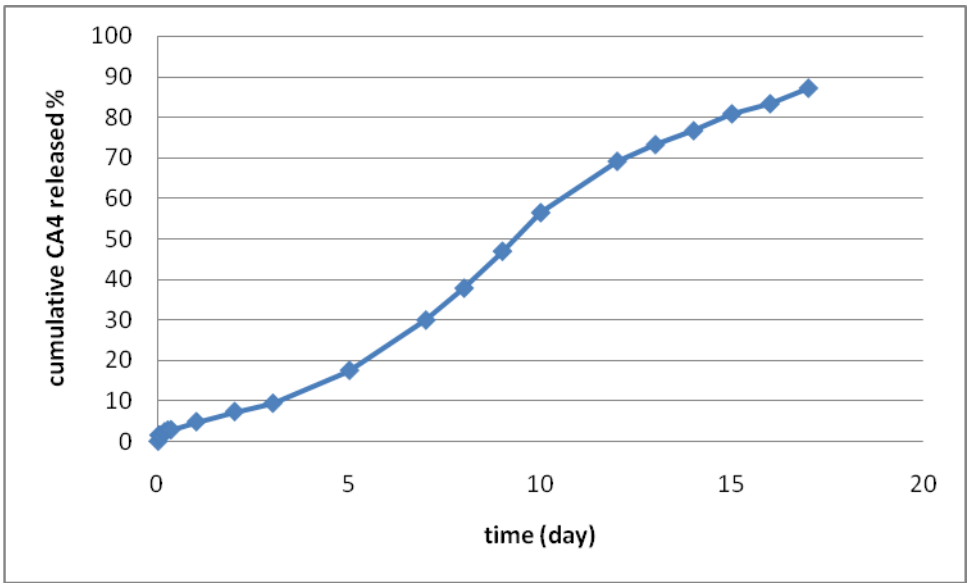

Figure 3.5: Cumulative *in vitro* CA4 released versus time for CA4 loaded PLGA NPs at 37 ºC

CA4 was encapsulated into biodegradable PLGA NPs by simple EEM. The small size of the obtained (around 200 nm) could be useful to achieve passive cancer-targeted drug delivery system throughout EPR effects. These CA4 loaded PLGA NPs showed an interesting long sustained release pattern of about 17 days to release most of the encapsulated CA4. In fact, this would permit the safe circulation of the NPs in the bloodstream without releasing a toxic dose of CA4 in the healthy tissue, but in the same time accumulates into the tumor tissue. In the same time, due to the size of these particles, they do not suffer kidney filtration as well as the free CA4 molecules, which permit to achieve a prolonged and controlled *in vivo* drug release.

Several kinetic models were analyzed to understand the release pattern of CA4 from the obtained CA4 loaded PLGA NPs. These models were zero order, zero order with T lag, first order, first order with T lag, Korsmeyer-

Peppas, Korsemeyer-Peppas with T lag, Higuchi model, Higuchi model with T lag, Hixon-Crowell, and Hixon-Crowell with T lag. The linear regression (R^2) and Akaike Information Criterion (AIC) were calculated [84-89] (Table 3.4).

Table 3.4: Release data modeling for CA4-PLGA NPs at pH 7.4 at 37˚C temperature.

release model	R^2	AIC
Zero order	0.9875	119.6777
Zero-order with T lag	0.9875	121.6696
First-order	0.9458	150.5285
First-order with T lag	0.9479	151.7116
Korsmeyer-Peppas	0.9889	119.1436
Korsmeyer-Peppas with T lag	0.9889	121.1490
Higuchi Model	0.8852	166.2972
Higuchi Model with T lag	0.9809	130.6295
Hixon-crowell	0.9602	144.6341
Hixon-Crowell with T lag	0.9631	145.0406

Understanding the release pattern can provide interesting information about the mechanisms involved in the release of CA4 from the obtained PLGA NPs. In fact, many release mechanisms such as diffusion through the pores or wall of the PLGA matrix, desorption of the drug from its surface, the disintegration of the PLGA NPs and subsequent release of CA4, and erosion and dissolution of the PLGA wall [90, 91].

The adopted model was based on the degree of fit of the linear regression (R^2) and the value of Akaike information criterion (AIC), which measure the goodness of fit based on maximum plausibility. Therefore, the most suitable model should demonstrate the lowest AIC and highest R^2 ($\approx$1).

Table 3.4 summarizes the outcome of the assessed release models and as can be seen, Korsmeyer-Peppas was adopted to describe the release mechanism of CA4 from our NPs, since it showed the highest R^2 (0.9889) and the lowest AIC (119.1436). This suggested mechanism is in agreement with the literature since the adopted kinetic model should demonstrate the similarity between observed and predicted release values [92]. In fact, this model is usually selected to describe the drug release behavior from PNPs, if the drug releases mechanism is not well-known or if there is more than one type of release mechanism involved in the manufactured system [93-95]. According to the literature, diffusion is the involved mechanism when the release exponent (n) is equal to 0.43. On the other hand, n values higher than 0.43 and lower than 0.85, suggesting an anomalous release that does not resemble Fick's Law. In addition, when the Value of n is lower than 0.43, a porous system, in which the release occurs by a combination of diffusion through the polymeric matrix and the pores. In this study the calculated n value was higher than 1 (about 1.120), which indicates that the release mechanism of CA4 is a Super case II transport; in fact, the value of n higher than 1 should mean an acceleration of the release in time, something similar control through PLGA erosion [96-100].

3.3.6 Stability study of CA4 loaded PLGA NPs

There was no significant variation in the observed particle size of NPs during the period of assessment which was conducted at the defined temperatures (Table 3.5).

Table 3.5: Size response in term of time for CA4 loaded PLGA NPs (A14) at the defined temperatures

Conditions	Day Zero	Day 1	Day 2	Day 3	Day 4
4°C	196.10 ± 5.09	196.83 ± 4.06	197.03 ± 5.17	202.13 ± 6.90	200.67 ± 5.91
25°C	193.63 ± 7.74	192.60 ± 8.73	192.13 ± 9.72	193.80 ± 4.71	193.53 ± 2.78

These results mean that the CA4 loaded PLGA NPs are kinetically stable for *in vivo* application during 4 days.

3.3.7 Anticancer activity

Caco-2 and HeLa cells were used to investigate the therapeutic efficacy of free CA4, free NPs, and charged NPs. Free cells without treatments where used as controls. The MTT cell viability assay was used to investigate the therapeutic effectiveness of free CA4, free NPs, and charged NPs. In addition, different concentrations of the free drug and the free and charged NPs were used in order to calculate the IC_{50}.

Regarding the activity of the free CA4 and the obtained charged NPs against Caco-2 cell line, it was found a strong and significant correlation between the free CA4 and the charged NPs since was close to 0.978 and p-value was less than 0.05. In addition, figure 3.6 showed a difference in the calculated IC_{50} between these two products with an IC_{50} close to 24.5 ng/ml for free CA4 and 4 ng/ml for the charged NPs. Moreover, the results of *in vitro* cytotoxicity showed that no significant effect was obtained after 24 hrs of treatment neither for the free drug nor for the charged NPs,

whoever both products showed their activity after 48 hrs of incubation (Figure 3.6).

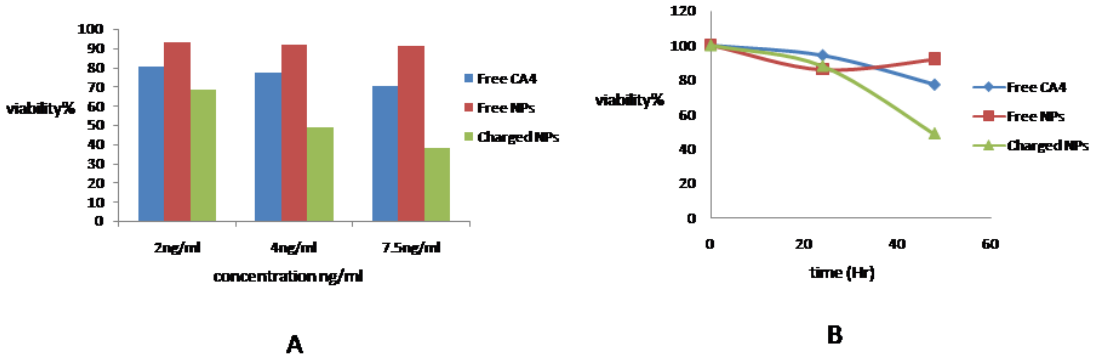

Figure 3.6: A. The therapeutic efficacy of free CA4, frees NPs, and charged NPs at different concentrations (2, 4, and 7.5) ng/ml. B. The time response relationship of free CA4, free NPs and charged NPs at 4 ng/ml.

Regarding the activity of the free CA4 and the obtained NPs against HeLa cell line, it was found a strong and significant correlation between the free CA4 and the charged NPs, since it was close to 0.995 and p-value was equal to 0.005. Furthermore, figure 3.7 showed a difference in the calculated IC_{50} between these two products with an IC_{50} close to 8 ng/ml for free CA4 and 2.5 ng/ml for the charged NPs. Moreover, the results of *in vitro* cytotoxicity showed that no significant effect was obtained after 24 hrs of treatment neither for the free drug nor for the charged NPs. However, both products showed marked activity after 48 hrs of incubation (Figure 3.7).

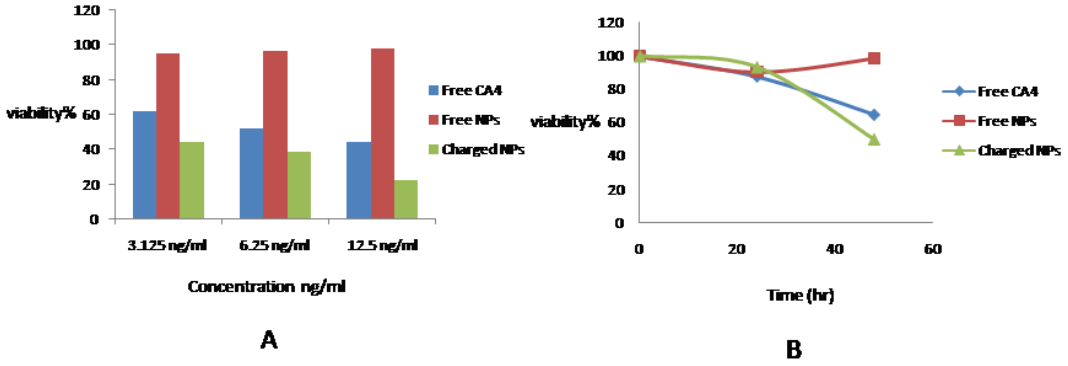

Figure 3.7: A. The therapeutic efficacy of free CA4, free NPs, and charged NPs at different concentrations (3.125, 6.25, and 12.5) ng\ml. B. The time response relationship of free CA4, free NPs and charged NPs at 2.5 ng\ml.

In fact, the free (uncharged) NPs showed no cytotoxic effect on the cultured cell lines. This suggests that producing CA4 loaded PLGA PNPs would improve the anticancer effect of CA4. In addition, the obtained NPs would cause fewer side effects due to the targeting and release pattern of these NPs.

Conclusion

The EEM was successfully used to produce the desired PLGA NPs since they had a particle size less than 200 nm which is the limit for opsonization by phagocytes. In addition, they were stable since their size remained constant for 4 consecutive days of incubation at 4 and 25˚C. In addition, they had satisfactory EE%. However, more trials could be run in order to improve this property. The obtained NPs were almost spherical in shape with a relatively smooth surface. The *in vitro* release showed an interesting long sustained release pattern of about 17 days required to release most of the encapsulated CA4. This would permit the safe circulation of the NPs in the bloodstream without releasing a toxic dose of CA4 in the healthy tissue, but in the same time accumulates into the tumor tissue. Korsmeyer-Peppas was adopted to describe the release mechanism of CA4 from our NPs since it showed the highest R^2 and the lowest AIC. Moreover, the calculated n value was higher than 1, which indicates that the release mechanism of CA4 is a Super case II transport.

Furthermore, these NPs were showed better cytotoxic results on two cell lines, Caco2 and HeLa, when compared with the free CA4. These results suggest that formulating CA4 in PLGA NPs would be of great importance in order to improve the safety and efficacy of this interesting cytotoxic drug. However, *in vivo* studies using animal models should be conducted in order to confirm these results.

Future work

Additional trials may be conducted using other formulation variables may be conducted in order to further decrease the particle size and increase the EE%. Also, *in vivo* studies on animals with tumors may be conducted in order to prove the effectiveness and safety of these NPs.

Limitations

Lack of some instruments such as probe sonicator, zeta sizer and NMR were the main obstacles to this kind of research.

References

1. Organization, W.H., ***estimated cancer incidence, mortality and prevelance wordwide in 2012,*** **in** ***cancer***2015, see http://www.who.int/cancer/en/.
2. McGuire, S., ***World cancer report 2014. Geneva, Switzerland: World Health Organization, international agency for research on cancer, WHO Press, 2015***. **Advances in Nutrition: An International Review Journal,** 2016. **7**(2): p. 418-419.
3. http://www.who.int/cancer/en/.
4. Putnam, D. and J. Kopeček, ***Polymer conjugates with anticancer activity,*** **in** ***Biopolymers Ii*****.** 1995, Springer. p. 55-123.
5. Organization, W.H., ***estimated cancer incidence, mortality and prevelance wordwide in 2012, in cancer***. 2015, see http://www.who.int/cancer/en/.
6. Allen, T.M., ***Ligand-targeted therapeutics in anticancer therapy.*** **Nature Reviews Cancer,** 2002. **2**(10): p. 750.
7. Ventola, ***C.L.T.n.r.P.E.c.P.a.T., 37***(9), 512.
8. Bonelli, P., et al., ***Ibuprofen delivered by poly (lactic-co-glycolic acid)(PLGA) nanoparticles to human gastric cancer cells exerts antiproliferative activity at very low concentrations.*** **International journal of nanomedicine,** 2012. **7**: p. 5683.
9. Akbarzadeh, A., et al., ***Liposome: classification, preparation, and applications.*** **Nanoscale research letters,** 2013. **8**(1): p. 102.

10. Miladi, K., et al., ***Nanoprecipitation process: from particle preparation to in vivo applications*****,* in *Polymer Nanoparticles for Nanomedicines*.** 2016, Springer. p. 17-53.
11. Chan, J.M., et al., ***Polymeric nanoparticles for drug delivery*****,* in *Cancer Nanotechnology*.** 2010, Springer. p. 163-175.
12. Duncan, R., ***Polymer conjugates as anticancer nanomedicines.*** **Nature reviews cancer**, 2006. **6**(9): p. 688.
13. Wilczewska, A.Z., et al., ***Nanoparticles as drug delivery systems.*** **Pharmacological reports,** 2012. **64**(5): p. 1020-1037.
14. De Jong, W.H. and P.J. Borm, ***Drug delivery and nanoparticles: applications and hazards.*** **International journal of nanomedicine, 2008. 3**(2): p. 133.
15. De Volder, M.F., et al., ***Carbon nanotubes: present and future commercial applications.*** **science,** 2013. **339**(6119): p. 535-539.
16. Bianco, A., K. Kostarelos, and M. Prato, ***Applications of carbon nanotubes in drug delivery.*** **Current opinion in chemical biology, 2005. 9**(6): p. 674-679.
17. Digge, M., R. Moon, and S. Gattani, ***Applications of carbon nanotubes in drug delivery: a review.*** **International Journal of PharmTech Research,** 2012. **4**(2): p. 839-847.
18. Ahmad, Z., et al., ***Polymeric micelles as drug delivery vehicles.*** **Rsc Advances,** 2014. **4**(33): p. 17028-17038.

19. Lee, M., et al., ***Size control of self-assembled nanoparticles by an emulsion/solvent evaporation method.*** **Colloid and Polymer Science, 2006. 284**(5): p. 506-512.
20. Nagavarma, B., et al., ***Different techniques for preparation of polymeric nanoparticles-a review.*** **Asian J. Pharm. Clin. Res,** 2012. **5**(3): p. 16-23.
21. Hornig, S., et al., ***Synthetic polymeric nanoparticles by nanoprecipitation.*** **Journal of Materials Chemistry,** 2009. **19**(23): p. 3838-3840.
22. Leo, E., et al., ***Polymeric nanoparticles as drug controlled release systems: a new formulation strategy for drugs with small or large molecular weight.*** **Journal of nanoscience and nanotechnology,** 2006. **6**(9-10): p. 3070-3079.
23. Banik, B.L., P. Fattahi, and J.L. Brown, ***Polymeric nanoparticles: the future of nanomedicine.*** **Wiley Interdisciplinary Reviews: Nanomedicine and Nanobiotechnology,** 2016. **8**(2): p. 271-299.
24. Masood, F., ***Polymeric nanoparticles for targeted drug delivery system for cancer therapy.*** **Materials Science and Engineering: C, 2016. 60**: p. 569-578.
25. Makadia, H.K. and S.J. Siegel, ***Poly lactic-co-glycolic acid (PLGA) as biodegradable controlled drug delivery carrier.*** **Polymers, 2011. 3**(3): p. 1377-1397.
26. Kapoor, D.N., et al., *PLGA:* ***a unique polymer for drug delivery.*** **Therapeutic delivery, 2015. 6**(1): p. 41-58.

27. Mallakpour, S. and V. Behranvand, ***Polymeric nanoparticles: Recent development in synthesis and application.*** **Express Polymer Letters, 2016. 10**(11): p. 895.

28. Astete, C.E. and C.M. Sabliov, ***Synthesis and characterization of PLGA nanoparticles.*** **Journal of Biomaterials Science, Polymer Edition, 2006**. **17**(3): p. 247-289.

29. Piñón-Segundo, E., M. G Nava-Arzaluz, and D. Lechuga-Ballesteros, ***Pharmaceutical polymeric nanoparticles prepared by the double emulsion-solvent evaporation technique.*** **Recent patents on drug delivery & formulation,** 2012. **6**(3): p. 224-235.

30. Rathbone, M.J., J. Hadgraft, and M.S. Roberts, **Modified-release drug delivery technology.** 2002: CRC Press.

31. Matsuo, M., et al., ***Delayed-release tablets using hydroxyethylcellulose as a gel-forming matrix.*** **International journal of Pharmaceutics,** 1996. **138**(2): p. 225-235.

32. Tajiri, S., et al., ***Dosage form design and in vitro/in vivo evaluation of cevimeline extended-release tablet formulations.*** **International journal of pharmaceutics,** 2010. **383**(1-2): p. 99-105.

33. Deshpande, A., et al., ***Controlled-release drug delivery systems for prolonged gastric residence: an overview.*** **Drug Development and Industrial Pharmacy,** 1996. **22**(6): p. 531-539.

34. Park, K., ***Controlled drug delivery systems: past forward and future back.*** **Journal of Controlled Release,** 2014. **190**: p. 3-8.

35. Siepmann, J., R. Siegel, and F. Siepmann, **Diffusion Controlled Drug Delivery Systems, in Fundamentals and Applications of Controlled Release Drug Delivery**, J. Siepmann, R.A. Siegel, and M.J. Rathbone, Editors. 2012, Springer US. p. 127-152.
36. Salsa, T., F. Veiga, and M. Pina, ***Oral controlled-release dosage forms. I. Cellulose ether polymers in hydrophilic matrices.*** **Drug Development and Industrial Pharmacy**, 1997. **23**(9): p. 929-938.
37. Jantzen GM, R.J., S**ustained and controlledrelease drug delivery systems, in Banker GS, Rhodes CT (Eds.) Modern Pharmaceutics,** Third Edition, Revised and Expanded, Drugs and the Pharmaceutical Sciences, vol 72, Marcell Dekker, Inc. New York, 1995: 575-609.hydrophobic polymers.
38. Zuleger, S.a.B.C.L., ***Polymer particle erosion controlling drug release. I. Factors influencing drug release and characterization of the release mechanism.*** **International Journal of Pharmaceutics,** 2001. 217(1–2): p. 139-152.
39. Borgquist, P., et al., ***A model for the drug release from a polymer matrix tablet—effects of swelling and dissolution.*** **Journal of controlled release,** 2006. **113**(3): p. 216-225.
40. Herrlich, S., et al., ***Osmotic micropumps for drug delivery.*** **Advanced drug delivery reviews,** 2012. **64**(14): p. 1617-1627.
41. Jaskari, T., et al., ***Controlled transdermal iontophoresis by ion-exchange fiber.*** **Journal of controlled release,** 2000. **67**(2-3): p. 179-190.

42. Borrel, C., et al., ***New antitubulin derivatives in the combretastatin A4 series: synthesis and biological evaluation.*** **Bioorganic & medicinal chemistry, 2005. 13**(11): p. 3853-3864.

43. Chen, H., et al., ***Design and synthesis of cyclopropylamide analogues of combretastatin-A4 as novel microtubule-stabilizing agents.*** **Journal of medicinal chemistry**, 2013. **56**(3): p. 685-699.

44. Young, S.L. and D.J. Chaplin, ***Combretastatin A4 phosphate: background and current clinical status.*** **Expert opinion on investigational drugs,** 2004. **13**(9): p. 1171-1182.

45. Medarde, M., A.B. Maya, and C. Pérez-Melero, ***Naphthalene combretastatin analogues: synthesis, cytotoxicity and antitubulin activity.*** **Journal of enzyme inhibition and medicinal chemistry,** 2004. **19**(6): p. 521-540.

46. Tozer, G.M., et al., ***The biology of the combretastatins as tumour vascular targeting agents.*** **International journal of experimental pathology**, 2002. **83**(1): p. 21-38.

47. Kanthou, C. and G.M. Tozer, ***The tumor vascular targeting agent combretastatin A–4-phosphate induces reorganization of the actin cytoskeleton and early membrane blebbing in human endothelial cells.*** Blood, 2002. **99**(6): p. 2060-2069.

48. Tarade, D., et al., ***Structurally simplified biphenyl combretastatin A4 derivatives retain in vitro anti-cancer activity dependent on mitotic arrest***. PloS one, 2017. **12**(3): p. e0171806.

49. Ma, M., et al., ***Synthesis and biological evaluation of Combretastatin A-4 derivatives containing a 3'-O-substituted carbonic ether moiety as potential antitumor agents.*** **Chemistry Central Journal,** 2013. **7**(1): p. 179.

50. Su, M., et al., ***The anti-angiogenic effect and novel mechanisms of action of Combretastatin A-4.*** **Scientific reports, 2016. 6: p. 28139.**

51. Quayle, L.A., et al., ***Anti-angiogenic drugs: direct anti-cancer agents with mitochondrial mechanisms of action.*** **Oncotarget,** 2017. **8**(51): p. 88670.

52. Rajak, H., et al., ***Design of combretastatin A-4 analogs as tubulin targeted vascular disrupting agent with special emphasis on their cis-restricted isomers.*** **Current pharmaceutical design,** 2013. **19**(10): p. 1923-1955.

53. Gaspari, R., et al., ***Structural basis of cis-and trans-combretastatin binding to tubulin.*** **Chem,** 2017. **2**(1): p. 102-113.

54. Sherbet, G., ***Suppression of angiogenesis and tumour progression by combretastatin and derivatives.*** **Cancer letters,** 2017. **403**: p. 289-295.

55. Rastogi, S.K., et al., ***Photoresponsive azo-combretastatin A-4 analogues.*** **European journal of medicinal chemistry,** 2018. **143**: p. 1-7.

56. Song, M.-Y., et al., ***Constructing novel dihydrofuran and dihydroisoxazole analogues of isocombretastatin-4 as tubulin***

polymerization inhibitors through [3+ 2] reactions. **Bioorganic & medicinal chemistry,** 2017. **25**(20): p. 5290-5302.

57. Ou, Y., et al., ***Combretastatin A4/poly (L-glutamic acid)-graft-PEG conjugates self-assembled to nanoparticles.*** **Asian Journal of Pharmaceutical Sciences,** 2017.
58. Zheng, S., et al., ***Design, synthesis, and biological evaluation of novel pyridine-bridged analogues of combretastatin-A4 as anticancer agents.*** **Journal of medicinal chemistry,** 2014. **57**(8): p. 3369-3381.
59. Stefański, T., et al., ***Design, synthesis, and biological evaluation of novel combretastatin A-4 thio derivatives as microtubule targeting agents.*** **European journal of medicinal chemistry,** 2018. **144**: p. 797-816.
60. Gaukroger, K., et al., ***Novel syntheses of cis and trans isomers of combretastatin A-4.*** **The Journal of organic chemistry**, 2001. **66**(24): p. 8135-8138.
61. Assali M, Z., A. N., Kittana, N., Hamad, D., & Amer, J. (2018). **Covalent Functionalization of SWCNT with Combretastatin A4 for Cancer Therapy.** Nanotechnology.2018 Jun 15;29(24):245101.
62. Wang, Y., et al., ***Targeted polymeric micelle system for delivery of combretastatin A4 to tumor vasculature in vitro.*** **Pharmaceutical research,** 2010. **27**(9): p. 1861-1868.

63. Wang, Z. and P.C. Ho, ***Self-Assembled Core–Shell Vascular-Targeted Nanocapsules for Temporal Antivasculature and Anticancer Activities.*** **Small**, 2010. **6**(22): p. 2576-2583.

64. Wang, Z., W.-K. Chui, and P.C. Ho, ***Nanoparticulate delivery system targeted to tumor neovasculature for combined anticancer and antiangiogenesis therapy.*** **Pharmaceutical research,** 2011. **28**(3): p. 585-596.

65. Wang, Y., et al., ***pH-sensitive pullulan-based nanoparticle carrier of methotrexate and combretastatin A4 for the combination therapy against hepatocellular carcinoma.*** **Biomaterials,** 2013. **34**(29): p. 7181-7190.

66. Sumer Bolu, B., E. Manavoglu Gecici, and R. Sanyal, ***Combretastatin A-4 conjugated antiangiogenic micellar drug delivery systems using dendron–polymer conjugates.*** **Molecular pharmaceutics,** 2016. **13**(5): p. 1482-1490.

67. Zaid, A.N., et al., ***Covalent Functionalization of SWCNT with Combretastatin A4 for Cancer Therapy.*** **Nanotechnology,** 2018.

68. Xiao C-F, Z.Y., Du J-L, Sun H-Y and Liu X-K 2012 **Hydroxyl substitutional effect on selective synthesis ofcis, transStilbenes and 3-Arylcoumarins through Perkin condensation Synth**. Commun. 42 1243–58.

69. Ghani, A., et al. (2014). **"Artificial Autotetraploidy Induction Possibility of Two Iranian Endemic Mint."** Not SciBiol 6(2): 185-195.

70. Pettit, G.R.S.B.S.B.M.R.H., E. (1995), "***Antineoplastic Agents. 291. Isolation and Synthesis of Combretastatins A-4, A-5, and A-6"*, Journal of Medicinal Chemistry,** 38: 1666–1672, doi:10.1021/jm00010a011.

71. Hussein, A.S., N. Abdullah, and A. Fakru'l-razi, ***Optimizing the process parameters for encapsulation of linamarin into PLGA nanoparticles using double emulsion solvent evaporation technique.*** **Advances in Polymer Technology,** 2013. **32**(S1).

72. Yao J, L.Y., Sun X, Dahmani FZ, Liu H, et al. ***Nanoparticle delivery and combination therapy of gambogic acid and all-trans retinoic acid.*** **Int J Nanomedicine. 2**014;9:3313–3324. [PMC free article] [PubMed].

73. Zhao X, C.Q., Liu W, Li Y, Tang H, et al. ***Codelivery of doxorubicin and curcumin with lipid nanoparticles results in improved efficacy of chemotherapy in liver cancer.*** **Int J Nanomedicine.** 2015;10:257–270. [PMC free article] [PubMed].

74. Narayanan S, P.M., Viswanath A, Narayanan D, Mohan CC, et al. ***Sequentially releasing dual-drug-loaded PLGA-casein core/shell nanomedicine: design, synthesis, biocompatibility and pharmacokinetics.*** **Acta Biomater.** 2014;10:2112–2124. [PubMed].

75. Arshad A, Y.B., Bienemann AS, Barua NU, Wyatt MJ, et al. ***Convection-Enhanced Delivery of Carboplatin PLGA Nanoparticles for the Treatment of Glioblastoma. PLoS One.*** 2015;10:e0132266. [PMC free article] [PubMed].

76. Huang J, Z.H., Yu Y, Chen Y, Wang D, et al. ***Biodegradable self-assembled nanoparticles of poly (D,L-lactide-co-glycolide)/hyaluronic acid block copolymers for targeted delivery of docetaxel to breast cancer.*** **Biomaterials.** 2014;35:550–566. [PubMed].

77. Muntimadugu E, K.R., Saladi S, Rafeeqi TA, Khan W. ***CD44 targeted chemotherapy for co-eradication of breast cancer stem cells and cancer cells using polymeric nanoparticles of salinomycin and paclitaxel.*** **Colloids Surf B Biointerfaces.** 2016;143:532–546. [PubMed].

78. Valencia PM, P.E., Perea B, Gadde S, Sweeney C, et al. ***Synergistic cytotoxicity of irinotecan and cisplatin in dual-drug targeted polymeric nanoparticles.*** **Nanomedicine (Lond)** 2013;8:687–698. [PMC free article] [PubMed].

79. Xiong H, Z.D., Qi Y, Zhang Z, Xie Z, et al. ***Doxorubicin-Loaded Carborane-Conjugated Polymeric Nanoparticles as Delivery System for Combination Cancer Therapy.*** **Biomacromolecules.** 2015;16:3980–3988. [PubMed].

80. Saha C, K.A., Das A, Pal S, Majumder D. A***nthracycline Drugs on Modified Surface of Quercetin-Loaded Polymer Nanoparticles:*** **A Dual Drug Delivery Model for Cancer Treatment.** PLoS One. 2016;11:e0155710. [PMC free article] [PubMed].

81. Sharma N, M.P., Lin S. ***Effect of process and formulation variables on the preparation of parenteral paclitaxel-loaded biodegradable***

polymeric nanoparticles: A co-surfactant study. **Asian J Pharm Sci.** 2016;11:404–416.

82. Bohrey, S., V. Chourasiya, and A. Pandey, ***Polymeric nanoparticles containing diazepam: preparation, optimization, characterization, in-vitro drug release and release kinetic study.*** **Nano convergence,** 2016. **3**(1): p. 3.
83. Jana, U., et al., ***Felodipine loaded PLGA nanoparticles: preparation, physicochemical characterization and in vivo toxicity study.*** **Nano Convergence,** 2014. **1**(1): p. 31.
84. Colombo, P., et al., ***Drug diffusion front movement is important in drug release control from swellable matrix tablets.*** **Journal of Pharmaceutical Sciences,** 1995. 84(8): p. 991-997.
85. Colombo, G., et al., ***Prolonged duration local anesthesia with lipid–protein–sugar particles containing bupivacaine and dexamethasone.*** **Journal of Biomedical Materials Research Part A**, 2005. 75A(2): p. 458-464.
86. Costa, P.a.J.M.S.L., ***Modeling and comparison of dissolution profiles.*** **Eur J Pharm** Sci, 2001. 13(2): p. 123-33.
87. Ferrero, C., A. Muñoz-Ruiz, and M.R. ***Jiménez-Castellanos, Fronts movement as a useful tool for hydrophilic matrix release mechanism elucidation.*** **International Journal of Pharmaceutics,** 2000. 202(1–2): p. 21-28.
88. Hariharan, D., et al., ***Mathematical analysis of drug delivery from swellable systems with partial physical restrictions or impermeable***

coatings. **International Journal of Pharmaceutics,** 1994. 112(1): p. 47-54.

89. Ritger, P.L.a.N.A.P., **A simple equation for description of solute release II. Fickian and anomalous release from swellable devices. Journal of Controlled Release,** 1987. 5(1): p. 37-42.
90. Polakovič, M., et al., ***Lidocaine loaded biodegradable nanospheres: II. Modelling of drug release.*** **Journal of Controlled Release,** 1999. **60**(2–3): p. 169-177.
91. Schaffazick SR, G.S., Freitas LL, Pohlmann AR., ***Physicochemical characterization and stability of the polymeric nanoparticle systems for drug administration.*** **Química Nova,** 2003. **26**(5): p. 726-737.
92. Motulsky, H.J. and A. Christopoulos, ***Fitting Model to Biological Data Using Linear and Nonlinear Regression: A Practical Guide to Curve Fitting*****, 2003, Graphpad software Inc.** : San Diego.
93. Korsmeyer, R.W., et al., ***Mechanisms of solute release from porous hydrophilic polymers.*** **International Journal of Pharmaceutics,** 1983. **15**(1): p. 25-35.
94. Brannon-Peppas, L., ***Recent advances on the use of biodegradable microparticles and nanoparticles in controlled drug delivery.*** **International Journal of Pharmaceutics,** 1995. **116**(1): p. 1-9.
95. Korsmeyer RW, P.N., **Macromolecular and modeling aspects of swelling controlled systems, in Controlled release delivery systems,** M.S. Roseman TJ, Editor 1983, Marcel Dekker Inc: New York. p. 77-89.

96. Motulsky, H.J.a.A.C., ***Fitting Model to Biological Data Using Linear and Nonlinear Regression:*** **A Practical Guide to Curve Fitting,** 2003, Graphpad software Inc. : San Diego.

97. Korsmeyer, R.W., et al., ***Mechanisms of solute release from porous hydrophilic polymers.*** **International Journal of Pharmaceutics,** 1983. 15(1): p. 25-35.

98. Brannon-Peppas, L., R***ecent advances on the use of biodegradable microparticles and nanoparticles in controlled drug delivery.*** **International Journal of Pharmaceutics,** 1995. 116(1): p. 1-9.

99. Korsmeyer RW, P.N., **Macromolecular and modeling aspects of swelling controlled systems, in Controlled release delivery systems,** M.S. Roseman TJ, Editor 1983, Marcel Dekker Inc: New York. p. 77-89.

100. Dash S, M.P., Nath L, Chowdhury P. ***Kinetic modeling on drug release from controlled drug delivery systems.*** **Acta Pol Pharm.** 2010 May 1;67(3):217-3.

Appendix

Table 5.1: Calibration curve data of CA4 in ACN at 300 nm

Concentration of CA4 (µg/ml)	Absorbance
50	1.580
40	1.276
30	0.930
21	0.667
10.5	0.371
5.25	0.171

Table 5.2: Calibration curve data of CA4 in 1% SLS in PBS at 304 nm

Concentration of CA4 (µg/ml)	Absorbance
50	1.640
40	1.30
28	0.930
19.6	0.650
11.76	0.39
5.88	0.197
2.94	0.103

Table 5.3: In-vitro CA4 released data from PLGA PNPs in 1% SLS in PBS (PH=7.4) at 37°

Time (day)	Cumulative CA4 released %
0.021	1.31
0.042	1.27
0.083	0.97
0.17	2.11
0.25	2.44
0.33	3.08
1	6.17
1.33	5.27
2	7.90
3	9.57
5	18.17
6	22.96
7	31.37
8	39.37
9	47.85
10	57.07
10.30	58.27
12	69.66
13	73.49
13.38	73.53

14	76.82
15	80.35
15.30	81.64
16	83.39
17	86.55

Table 5.4: In-vitro cytotoxicity data of free CA4 and charged NPs on Caco-2 cells

Concentarion of CA4 in ng/ml	Viability % of Caco-2 cells treated with free CA4	Viability % of Caco-2 cells treated with Charged NPs
3.125	62.5	44.8
6.25	52.3	38.9
12.5	44.5	22.7

Table 5.5: In-vitro cytotoxicity data of free CA4 and charged NPs on HeLa cells

Concentarion of CA4 in ng/ml	Viability % of HeLa cells treated with free CA4	Viability % of HeLa cells treated with Charged NPs
3.125	80.4	68.5
6.25	77.4	49.0
12.5	70.4	37.8

كلية الدراسات العليا

جامعة النجاح الوطنية

تركيب و توصيف الجسيمات البولمريه بحجم النانو لمركب فعال ضد السرطان (كومبريتاستاتين)

إعداد

منى حسان

إشراف

أ. د. عبد الناصر زيد

د. علاءالدين الكيلاني

قدمت هذه الأطروحة استكمالاً لمتطلبات الحصول على درجة الماجستير في العلوم الصيدلانية بكلية الدراسات العليا في جامعة النجاح الوطنية في نابلس، فلسطين.

2018

تركيب و توصيف الجسيمات البولمريه بحجم النانو لمركب فعال ضد السرطان (كومبريتاستاتين)

إعداد

منى حسان

إشراف

أ.د. عبدالناصر زيد

د. علاء الدين الكيلاني

الملخص

الخلفية: تكنولوجيا النانو الصيدلانية هي تكنولوجيا ناشئة أثبتت فعاليتها في تقليل الآثار الجانبية وتحسين النتائج العلاجية للأدوية الكيميائية. كومبريتاستاتين هو مستخلص طبيعي و عامل كيميائي قوي و فعال في قتل الخلايا السرطانية لكن أظهر سمية عالية على القلب.

الغرض: كان الهدف من هذا البحث هو صياغة و توصيف الجسيمات النانونية البولمرية وتقييم نمط تحرير الكومبريتاستاتين و تقييم سمية الجسيمات النانونية على الخلايا السرطانية. **الطريقة:** تم تصنيع الكومبريتاستاتين باستخدام تفاعل بيركن. تم استخدام طريقة الترسيب–النانوية و طريقة تبخر المستحلب لإنتاج الجسيمات النانونية المطلوبة. الجسيمات النانونية التي تم الحصول عليها تم توصيفها من حيث الشكل و حجم الجسيمات والجهد الكهربائي والنسبة المئوية لكفاءة التغليف والنسبة المئوية لتحميل الدواء و تحريره. كما تم أيضاً تحديد سميتها على نوعين من الخلايا السرطانية وهي كاكو–2 وهيلا.

النتائج: أثبت طريقة تبخر المستحلب قدره أفضل على إنتاج الجسيمات النانونية المحملة بالكومبريتاستاتين على شكل كروي مع كفاءة جيدة لحمل المركب (50.84%) ومتوسط حجم حوالي 203.25 نانوميتر. كما أنها أظهرت نمط تحرير طويل الأمد. تم اعتماد كورسماير–بيبابس لوصف آلية إطلاق الكومبريتاستاتين من الجسيمات النانونية التي لدينا مع قيمة ن أعلى من 1. أما بالنسبة للسمية الخلوية على خلايا الكاكو–2 و الهيلا فقد أظهرت الجسيمات النانوية المحملة بالكومبريتاستاتين سمية أفضل من الكومبريتاستاتين الحر على كلا الخلايا. **الخلاصة:** تم إنتاج

الجسيمات البولمرية النانونية المحملة بالكومبريتاستاتين بنجاح وأظهرت خصائص مرضية من حيث الحجم والشكل الكروي وكفاءة التحميل كما أظهرت نمط تحرير طويل الأمد و مستدام. بالإضافة إلى ذلك، أظهرت تحسن في السمية الخلوية مقارنة مع مادة الكومبريتاستاتين الحرة. هذا يشير إلى أن هذه الجسيمات النانونية يمكن استخدامها لتحسين سلامة وفعالية الكومبريتاستاتين. ومع ذلك يجب إجراء الدراسات على الحيوانات لإثبات هذه النتائج المثيرة للاهتمام.